Ph. D Thesis

SYNTHESIS AND CHARACTERIZATION OF AROMATIC POLYMERS FROM VANILLIN DERIVATIVES

Hong Sun

（Supervisor: Professor Kenji Ogino）

Graduate School of Bio-Applications and Systems Engineering

Tokyo University of Agriculture and Technology

March 2016

Content

Chapter 3 Synthesis and Characterization of Biobased Polyesters Derived From Vanillin-based Schiff Base and Cinnamic Acid Derivatives

Chapter 4 Radical Copolymerization of Ferulic Acid Derivatives with Ethylenic Monomers

Chapter 5 Conclusion

Acknowledgements

The author gratefully acknowledges his supervisor, Professor Kenji Ogino, who gave me the opportunity to study in Ph. D course, supervision, and research assistantships with endless patience. During these years in the Ogino laboratory, the author has studied a lot of knowledge from him. In addition, the supervisor also gave the author some help of life.

The author is also extremely grateful to the thesis committee members, Professor Munetaka Nakata, Professor Yoichi Tominaga, Professor Nobuyuki Akai, and Professor Susumu Inasawa (Tokyo University of Agriculture and Technology) for their invaluable comments and kind suggestions.

The author would like to thank Dr. Shinji Kanehashi for his thoughtful guidance and enlightening suggestions.

The author wants to thank Professor Hidehiro Kamiya, Professor Koji Nakano, Professor Keiichi Noguchi, who provided a great help on TG-DTA measurements, POM measurements, and HRMS ESI measurements, respectively.

The author also appreciates all the members in the Ogino research group, who make the author feel pleasure during studying and living. Specially, the author is thankful to Dr. Yuuki Miyazaki, Mr. Hiroshi Nakamura, Mr. Yaohui Wang and Mr. Qian Sicong for helping with the author's studies.

Chapter 1 General Introduction

1.1 Biomass-based Polymer Materials and Their Applications

Recently, environmental problems involving global warming, air/water pollution, depletion of fossil fuels resulting from highly energy demand owing to population growth and development of industry have been widely seen in our daily life. Energy conservation and use of clean energy sources such as hydrogen, solar power, and wind are one effective solution for these problems. Another strategy is the production of polymer materials from renewable resources. The use of bio-based polymer materials made from natural products, which are renewable resources involving plants and nonfood materials, is one of the most effective methods for addressing these environmental challenges.

The renewable polymers shown in Figure 1-1 contain biopolymers and polymers derived from bio-based monomers [1]. In recent years, the preparation of bio-based polymer materials with natural monomers has attracted lots of attention [2].

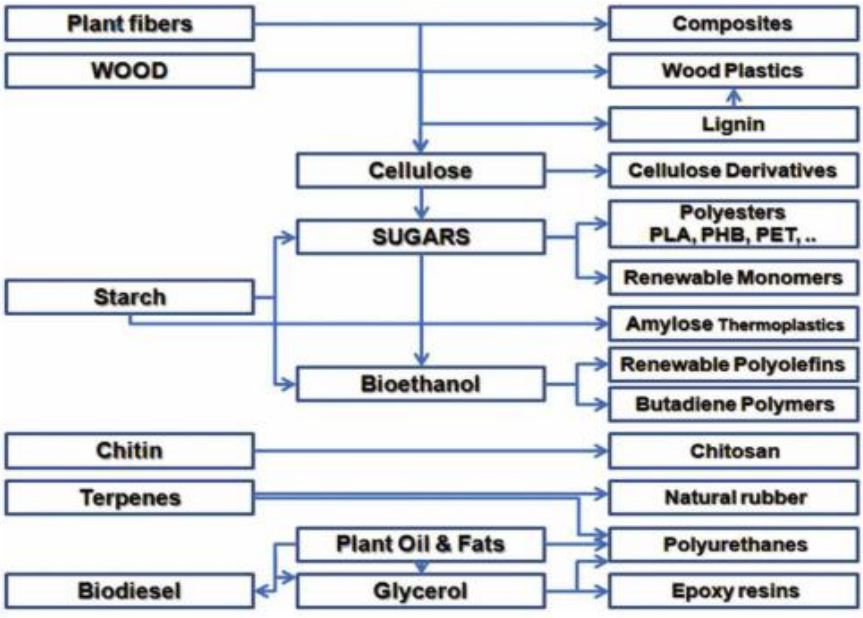

Figure 1-1 Renewable polymers based upon carbohydrates and terpenes

Bio-based polyesters have been synthesized from natural monomers which are derived from starch, cellulose, lignin and so on [3]. Poly (lactic acid) (PLA), a common, biodegradable thermoplastics derived from renewable plants, can be produced in two routes as shown in Figure 1-2. The common route is the ring-opening polymerization of lactide with metal catalysts [4-6]. Another route is the direct condensation of lactic acid monomers [7]. PLA has been used for a variety of biomedical applications such as pins, prosthetics, sutures, dental implants, vascular grafts, artificial skin, bone screws, stents, contraceptives, prostate cancer treatments and plates for temporary internal fracture fixation [8-17].

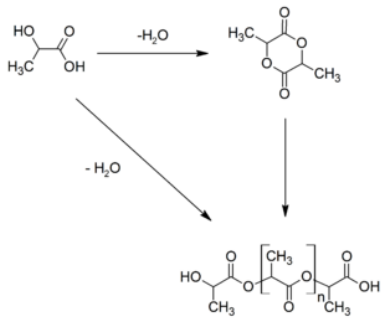

Figure 1-2 The synthetic routes of poly (lactic acid)

Poly(hydroxyalkanoates) (PHAs) originated from more than 150 different monomers have been completely synthesized by microorganisms with sugars or lipids. The structures and applications are shown in Figures 1-3 and 1-4, respectively.

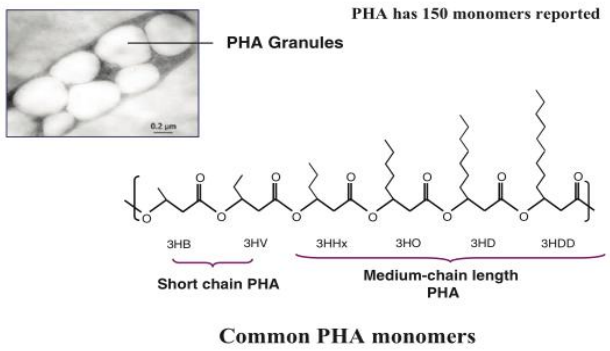

Figure 1-3 Structures of poly(hydroxyalkanoates) monomers [18]

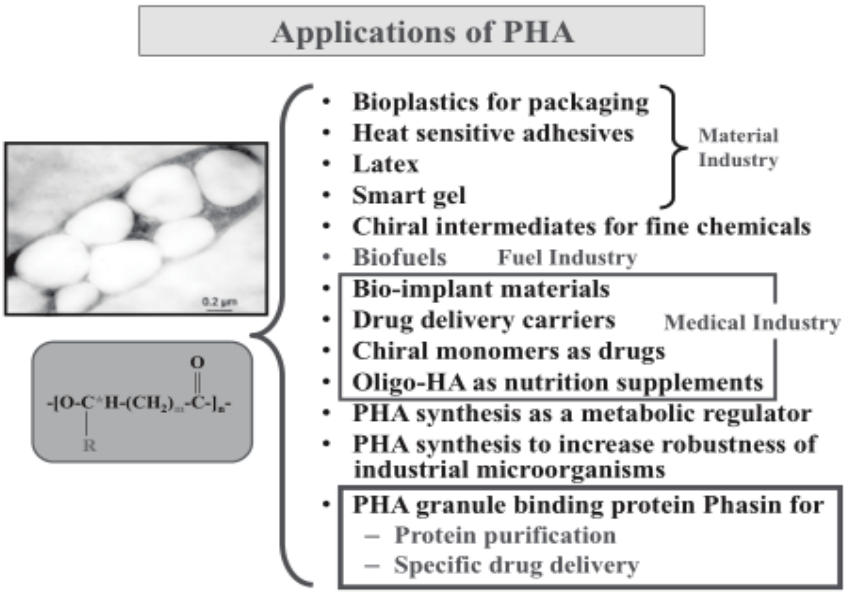

Figure 1-4 Applications of PHA [18]

Lignin is an aromatic polymer that makes up 15–30% of the cell walls of terrestrial plants [19]. It is one of the most promising renewable biomass, possessing some major chemical functional groups such as hydroxy, methoxy, and carbonyl groups. Hydroxy and

other chemical functional groups have played a major role in the chemical applications of lignin [20, 21]. There are a variety of chemical modifications for the utilization of lignin. Low molecular weight of degradation product of lignin can be also converted to epoxy resins [22]. Other examples for industrial products derived from lignin are reinforcements [23, 24], adhesives [25-27], adsorbents [28-30], flocculants [31-34] and an antioxidant additive [35-38].

Small molecules derived from lignin have been also studied in order to construct the useful bio-based materials. For example, 2-pyrone-4,6-dicarboxylic acid (PDC) is a chemically stable metabolic intermediate of lignin. PDC has been converted to polyesters, and anomalous adhesion properties as high as about 30–60 MPa against several metals have been reported [39].

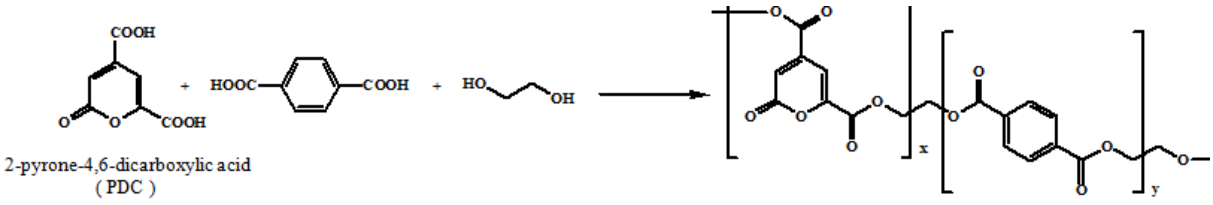

Figure 1-5 Preparation of polyester using PDC as a monomer [39]

Figure 1-6 represents chemical structure of renewable resources, vanillin, ferulic acid, and *p*-coumaric acid used in this work. Vanillin (Figure 1-6a), the raw material which is derived from lignin, can be produced from straw and rice bran by fermentation. It was successfully extracted from cow dung in National Center for Global Health and Medicine (NCGM) in 2007. It is an environmentally friendly product, and has several advantages such as low price, green chemical resource, and natural abundance [40].

Vanillin has been considered as one of the potential renewable resources and investigated to develop functional polymer materials in recent years [41, 42]. For example,

vanillin has been converted into thermosetting resins (*e.g.*, epoxy and phenolic) [43-45], polyesters [46,47], and acrylate/methacrylate polymers [48,49].

Ferulic acid (Figure 1-6b), another raw material, is a very important component for the biological functionality of the cell wall, as well as for the structural stability. It is reported that ferulic acid moieties are contained in cell wall polysaccharides through ester linkage, and they can be coupled oxidatively to form dimers leading to crosslinking of polysaccharide chains [50-52]. A wide range of applications have been proposed including as an antioxidant [53-56]. *Trans*-Coumaric acid (Figure 1-6c) is an intermediate metabolite of the biosynthesis by lignin [57]. Some studies have revealed that the *trans*-coumaric acid moiety shows photodimerization in its thermotropic phases [58-62]. Thermotropic liquid crystalline properties of homopolymer and its copolymer containing *trans*-Coumaric acid have also been reported [63].

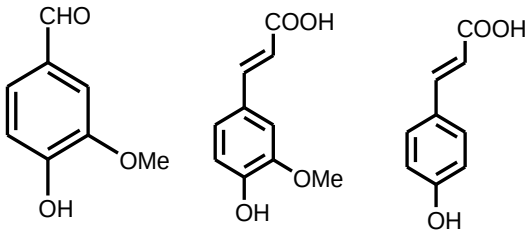

(a) (b) (c)

vanillin **ferulic acid** ***p*-coumaric acid**

Figure 1-6 Structure of natural renewable resources used in this work

1.2 Purpose and Outline of This Thesis

This thesis deals with the fundamental research for the development of functional bio-based polymer materials. Vanilin, ferulic acid, and coumaric acid are utilized as starting materials for polymer syntheses. High bio-based content, remarkable characteristics, and facile synthetic routes are taken into consideration in the molecular design of polymers. Since all of bio-based starting materials are aromatic compounds, polymers with rigid and tough natures are expected in the main chain type polymers. It is also expected that photochemical and photophysical functionalities are afforded to the polymers, which are difficult to be possessed by conventional bio-based polymers.

This thesis consists of five chapters.

Chapter 1 (this chapter) provides a general introduction of this thesis, including some background of environmental concern and current investigation of biomass-based polymer materials. For example, typical well-known bio-based polymers, poly(lactic acid) (PLA) and poly(hydroxyalkanoates) (PHA) as biodegradable polymers are introduced. In addition, key materials throughout this thesis, vanillin, ferulic acid, and *p*-coumaric acid are also shortly introduced. The purpose of this thesis is also described.

Chapter 2 provides synthesis and characterization of bio-based poly(ether benzoxazole) derived from vanillin. Poly(ether-*o*-hydroxyamide) (PEHA) precursor from a novel monomer which is derived from bio-based material, vanillin is prepared and the subsequent thermal cyclodehydration affords poly(ether-benzoxazole) (PEBO) as shown in Scheme 1-2. The structure analyses, solvent solubility, thermal stability, and mechanical properties of the PEHA precursor and PEBO are described.

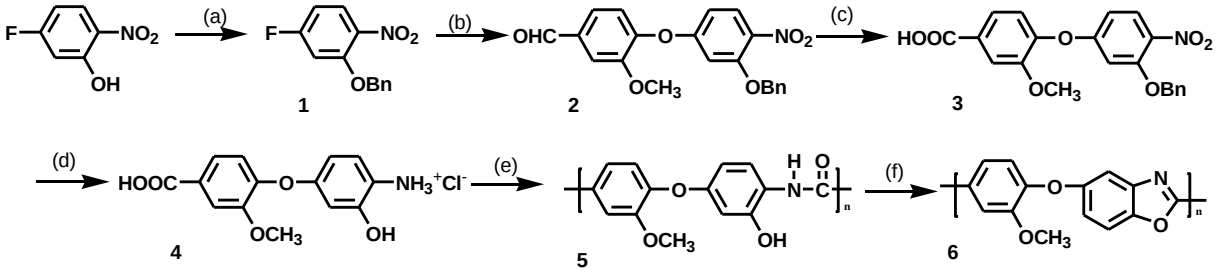

Scheme 1-1 Synthesis of PEBO. (a); BzBr, K_2CO_3, DMF, (b); Vanillin, K_2CO_3, 18-Crown-6, DMF, (c); $KMnO_4$, acetone, (d); palladium 10% on carbon (Pd-C), HCl, (e); DBOP, Et_3N, NMP, (f); thermal treatment, NMP.

Chapter 3 provides synthesis and characterization of all bio-based copolyesters derived from renewable resources, vanillin, ferulic acid, and *p*-coumaric acid. Compared with poly(ether benzoxazole) in Chapter 2, the higher bio-based content is fulfilled since novel vanillin-based Schiff base is used as a monomer. Monomer synthesis and polymerization via transesterification reactions are carried out to synthesize homo- and copolyesters with ferulic acid or coumaric acid as shown in Scheme 1-2.

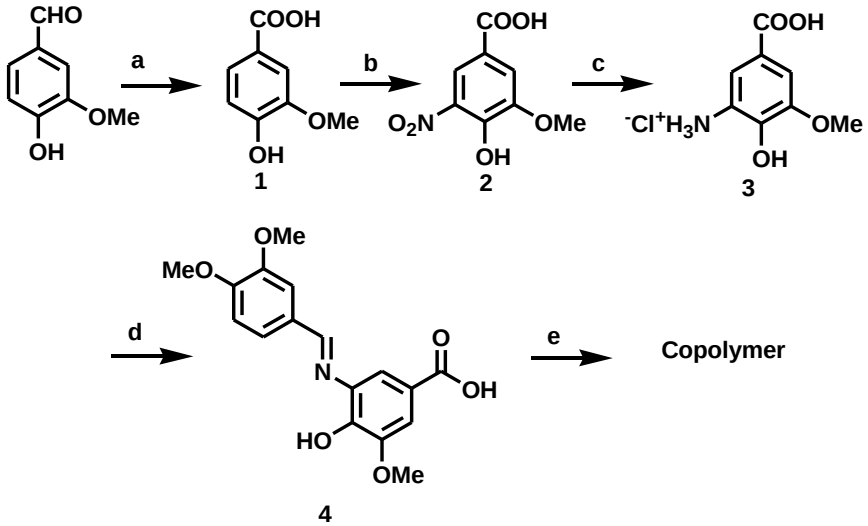

Scheme 1-2 Synthesis of 3-[(3,4-dimethoxybenzylidene)amino]-4-hydroxy-5 -methoxybenzoic acid (DAHMBA) and homo- and copolymers with *p*-coumaric acid and ferulic acid. (a); KOH, (b); HNO_3, AcOH, (c); Palladium on carbon (Pd/C, 10% loading), ethanol, HCl, H_2, (d); Veratraldehyde, ethanol, (e); *p*-Coumaric acid or ferulic acid, acetic anhydride, disodium hydrogen phosphate.

Chapter 4 provides radical copolymeriztion of ferulic acid derivatives with vinyl monomers. In Chapters 2 and 3, hydroxyl, formyl and carboxy groups are utilized for polymerization. Radical polymerization is one of the easiest ways to produce polymers. Copolymerization behaviors of ferulic acid modified monomer with styrene, methyl methacrylate and styrene derivative resulting from the decarbonation of ferulic acid are investigated as presented in Scheme 1-3.

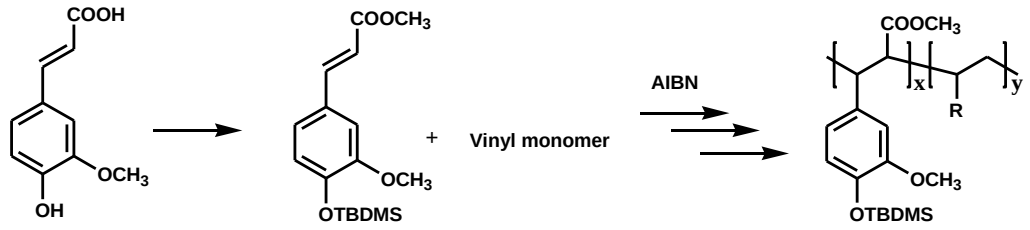

Scheme 1-3 synthesis of ferulic acid derivative copolymers with vinyl monomers

Finally, Chapter 5 is the conclusion of this thesis. The presented conclusion would facilitate the development of novel functional bio-based polymer materials.

1.3 References

1. Rolf, M. *Macromol. Chem. Phys.*, **2013**, 214, 159
2. Han, Y. M.; Qin, T. F.; Chu, F. X. 2012 International Conference on Biobase Material Science and Engineering (BMSE), China.
3. Corma, A.; Iborra, S.; Velty, A. *Chem. Rev.*, **2007**, 107, 2411.
4. Kowalski, A.; Duba, A.; Penczek, S. *Macromolecules*, **2000**, 33, 7359.
5. Kricheldorf, H. R.; Saunders, K. I.; Stricker, I. *Macromolecules*, **2000**, 33, 702.
6. Du, H.; Pang, X.; Yu, H. et al. *Macromolecules*, **2007**, 40, 1904.
7. Maharanaa, B.; Mohantyb, Y. S. *Prog. Polym. Sci.*, **2008**, 34, 99.
8. Frazza, E. J. and Schmitt, E. E. *J. Biomed. Mater. Res. Symp*. **1971**, 1, 43.
9. Williams, C. K. *Chem. Soc. Rev. ,* **2007**, 36, 1573.
10. Albertsson, A. C.; Varma, I. K. *Biomacromolecules*, **2003**, 4,1466.
11. Benicewicz, B. C.; Hooper, P. K. *J. Bioact. Compat. Polym.* **1990**, 5, 453.
12. Brady, J. M.; Cutright, D. E.; Miller, R. A., Battistone, G. C.; Hunsuck, E. E. *Biomed. Mater. Res*. **1973**, 7, 155.
13. Vainionpaa, S.; Rokkanen, P.; Tormala , P. *Prog. Polym. Sci.* **1989**, 14, 679.
14. Vert, M. *Angew. Makromol. Chem.* **1989**, 166/167, 155.
15. Gogolewski, S.; Pennings, A. J. *Makromol. Chem. Rapid Commun.* **1983**, 4, 675.
16. Korenthal, R. L. Biodegradable polymers in medicine and surgery. *Polymers in Medicine and Surgery*; Korenthal, R. L., Oser, Z., Martin, E., Eds.; Plenum Press: New York, **1975**; p 119.
17. Leenslag, J. W.; Pennings, A. J.; Bos, R. R. M.; Rozema, F. R.; Boering, G. *Biomaterials*, **1987**, 8, 311.
18. Chen, G.Q. Plastics completely synthesized by bacteria: polyhydroxyalkanoates, *Microbiology Monographs*, 2010; P17.
19. Elena, T.; Wilfred, V. *J. appl. polym. sci*., **2015**, 42069.

20. Lin, L.; Yoshioka, M.; Yao, Y.; Shiraishi, N. *J. Appl. Polym. Sci.*, **1994**, 52, 1629.

21. Whetten, R.; Sederoff. R. *The Plant Cell*, **1995**, *7*, 1001.

22. Tsunoda, T.; Oyama, T; Takahashi, A.; Kono, T., *Poly. Prep. Jpn.* **2010**, *59*, 3618.

23. Xiao, S.; Feng, J.; Zhu, J.; Wang, X.; Yi, C.; Su, S. *J. Appl. Polym. Sci*., **2013**, 130, 1308.

24. Frigerio, P.; Zoia, L.; Orlandi, M.; Hanel, T.; Castellani, L. *Bioresources*, **2014**, 9, 1387.

25. Effendi, A.; Gerhauser, H.; Bridgwater, A. V. *Renew. Sustain. Energy Rev.*, **2008**, 12, 2092.

26. Yuan, Y.; Guo, M.; Liu, F. *BioResources*, **2014**, 9, 836.

27. Qin, J.; Woloctt, M.; Zhang, J. *ACS Sustain. Chem. Eng*., **2014**, 2, 188.

28. Ciesielczyk, F.; Klapiszewski, Ł.; Szwarc-Rzepka, K.; Jesionowski, T. *Adv. Powder Technol*., **2014**, 25, 695.

29. Nowacka, M.; Klapiszewski, Ł.; Norman, M.; Jesionowski, T. *Cent. Eur. J. Chem*., **2013**, 11, 1860.

30. Fu, K.; Yue, Q.; Gao, B.; Sun, Y.; Zhu, L. *Chem. Eng. J*., **2013**, 228, 1074.

31. Bratby, J. Coagulation and Flocculation in Water and Wastewater Treatment, 2nd ed.; IWA Publishing: London, **2006**, p 401.

32. Lee, K. E.; Morad, N.; Teng, T. T.; Poh, B. T. *Chem. Eng. J*., **2012**, 203, 370.

33. Verma, A. K.; Dash, R. R.; Bhunia, P. *J. Environ. Manage*., **2012**, 93, 154.

34. Rong, H.; Gao, B.; Zhao, Y.; Sun, S.; Yang, Z.; Wang, Y.; Yue, Q.; Li, Q. *J. Environ. Sci.*, **2013**, 25, 2367.

35. Petersen, K.; Væggemose Nielsen, P.; Bertelsen, G.; Lawther, M.; Olsen, M. B.; Nilsson, N. H.; Mortensen, G. *Trends Food Sci. Technol*., **1999**, 10, 52.

36. Silvestre, C.; Duraccio, D.; Cimmino, S. *Prog. Polym. Sci*., **2011**, 36, 1766.

37. Arshanitsa, A.; Ponomarenko, J.; Dizhbite, T.; Andersone, A.; Gosselink, R. J.; Van der Putten, J.; Lauberts, M.; Telysheva, G. *J. Anal. Appl. Pyrolysis*, **2013**, 103, 78.

38. Johansson, K.; Winestrand, S.; Johansson, C.; Jarnstrom, L.; Jonsson, L. J. *J. Biotechnol*,

2012, 161, 14.

39. Hishida, M.; Shikinaka, K.; Katayama ,Y.; Kajita ,S.; Masai, E.; Nakamura, M.; Otsuka ,Y.; Ohara, S.; Shigehara, K. *Polym. J.,* **2009**, *41*, 297.
40. Bomgardner M. M. *Chem. Eng. News*, **2014**, 92, 6.
41. Ravikumara, L. et al, *Mater. Chem. Phys,* **2009**, *115***,** 632.
42. Fache, M.; Boutevin, B., Caillol, S. *Eur. Polym. J.*, **2015**, 68, 488.
43. Koike, T. *Polym. Eng. Sci.*, **2012**, 52, 701.
44. Aouf, C.; Lecomte, J.; Villeneuve, P.; Dubreucq, E.; Fulcrand, H. *Green Chem*., **2012,** 14, 2328.
45. Chauhan, N. P. S. *Des. Monomers Polym.*, **2012**, 15, 587.
46. Mialon, L.; Pemba, A. G.; Miller, S. A. *Green Chem*., **2010**, 12, 1704.
47. Mialon, L.; Vanderhenst, R.; Pemba, A. G.; Miller, S.A. *Macromol Rapid Commun*., **2011**, 32, 1386.
48. Stanzione III, J. F.; Sadler, J. M.; La Scala, J. J.; Reno, K. H.; Wool, R. P. *Green Chem*., **2012**, 14, 2346.
49. Holmberg, A. L.; Stanzione, J. F.; Wool, R. P.; Epps, T. H. *ACS Sust. Chem. Eng.*, **2014**, 2, 569.
50. Ishii, T. *Plant Sci*., **1997**, 127, 111.
51. Hartley, R.D. *Phytochemistry*, **1973**, 12, 661
52. Fry, S.C. *Annu. Rev. Plant Physiol*., **1986**, 37, 165.
53. Albertsson, A. C.; Varma, I. K. *Biomacromolecules,* **2003**, 4,1466.
54. Benicewicz, B. C.; Hooper, P. K. *J. Bioact. Compat. Polym.* **1990**, 5, 453.
55. Brady, J. M.; Cutright, D. E.; Miller, R. A., Battistone, G. C.; Hunsuck, E. E. *Biomed. Mater. Res*. **1973**, 7, 155.
56. Vainionpaa, S.; Rokkanen, P.; Tormala , P. *Prog. Polym. Sci.* **1989**, 14, 679.
57. Hernanz, D.; Nunez,V.; Sancho, A. I.; Faulds, C. B.; Williamson, G.; Bartolome, B.;

Gomez-Cordoves, C. *J.Agric. Food. Chem.*, **2001**, 49, 4884.

58. Jin, X.; Carfagna, C.; Nicolais, L.; Lanzetta, R. Macromolecules, **1995,** 28, 4785.
59. Griffin, A. C.; Hoyle, C. E.; Gross, J. R. D.; Venkataram, K.; Creed, D. *Makromol. Rapid Commun.*, **1988**, 9, 463.
60. Haddleton, D. M.; Creed, D.; Griffin, A. C.; Hoyle, C. E.; Venkataram, K. *Makromol. Rapid Commun.*, **1989**, 10, 391.
61. Kawatsuki, N.; Suehiro, C.; Yamamoto, T. *Macromolecules,* **1998,** 31, 5984.
62. Yang, J.; Wegner, G. *Macromolecules*, **1992**, 25, 1791.
63. Kaneko, T.; Hang, T. T.; Matsusaki, M.; Akashi, *M. Chem. Mater.*, **2006,** 18, 6220.

Chapter 2 Synthesis and Characterization of Bio-based Poly(Ether Benzoxazole) Derived From Vanillin

Abstract

The synthesis of bio-based poly(ether benzoxazole) (PEBO) derived from natural product vanillin was investigated. Poly(ether *o*-hydroxy amide) (PEHA) was used as a precursor of PEBO. PEBO was obtained by thermal treatment of PEHA based on the cyclodehydration. Synthesized PEBO was analyzed by Fourier transform infrared spectrometry (FTIR), differential scanning calorimetry (DSC) and thermogravimetric analysis (TGA) to confirm the structure and thermal properties. The resultant PEBO film showed flexible and self-standing property. This film also had 5.2 GPa for Young's modulus and 117 MPa for tensile strength which were higher than those of the commercial engineering polymers and other PEBOs.

2.1 Introduction

Aromatic poly(*p*-phenylene benzobisoxazole) (PBO) is a class of heterocyclic polymers with excellent thermal stability, high mechanical strength, high elastic modulus, and flame retardance [1-3]. Therefore, PBOs have been commercialized to thermal and mechanical resistance materials for electronic materials, structure additives, and high-strength clothes. The commercial PBO fiber (Zylon^{TM}) produced by Toyobo Co., Ltd, Japan, is induced to prepare highly-oriented fiber and shows excellent properties as mentioned-above [4, 5]. However, poor processability resulting from the sparingly solubility in organic solvents and high melting point of PBO limit its further applications. One possible approach to prepare PBO is the use of strong acids, such as poly(phosphoric acid) (PPA) and sulfuric acid (H_2SO_4), which dissolve PBO [6, 7]. However, the use of such an acid is environmentally unfriendly and unfavorable in view of manufacturing [8, 9]. Residual PPA also reduces mechanical properties [10]. Another strategy to prepare PBO is the use of thermal transformation of a poly(*o*-hydroxyamide) (PHA) [11-13] or poly (hydroxyl imide) [14-16] precursor for cyclization to form a benzoxazole structure. This thermal transformation process usually leads to possible crosslinking during the rearrangement of the chemical structure, indicating that the solubility of these polymers is also still very limited. Flexible units or bulky pendant groups attach to the backbone to improve their solubility and/or melt processability [17-25]. For example, incorporation of ether linkage in the polymer backbone improves solubility with retaining their thermal properties.

Recently, biomass-based polymer materials derived from renewable resources such as plant and non-food products have received much attention because of the increasing price of petrochemical products, its depletion, and growing environmental concerns [26]. The use of natural renewable resources would be one effective solution for this concern and beneficial in the development of novel environmentally-friendly polymer materials. Vanillin, 4-hydroxy-3-methoxybenzaldehyde, is one of the renewable resources since it can be produced from lignin

through the sustainable process such as controlled oxidation [27]. Therefore lignin derived vanillin can be a promising feedstock chemical for the polymer industries as well as for the food and pharmaceutical industries. Although several polymers have been synthesized with vanillin and its derivatives as building block [28-35], there is no report about the thermally and mechanically high performance polymers like PBOs.

In this chapter, the author reports synthesis of poly(ether-*o*-hydroxyamide) (PEHA) precursor from a novel monomer which is derived from bio-based material, vanillin and the thermal cyclodehydration to afford poly(ether benzoxazole) (PEBO). The structure analyses, solvent solubility, thermal stability, and mechanical properties of the PEHA precursor and PEBO are described.

2.2 Experimental Section

2.2.1 Materials

Tetrahydrofuran (THF) was used as distilled over sodium and benzophenone. The following reagents and solvents were used as received; 5-fluoro-2-nitrophenol (Tokyo Chemical Industry. Co. Ltd.), benzyl bromide (Wako Pure Chemical Industries, Ltd.), dimethylformamide (DMF) (Wako Pure Chemical Industries, Ltd.), potassium carbonate (Wako Pure Chemical Industries, Ltd.), vanillin (Wako Pure Chemical Industries, Ltd.), 1,4,7,10,13,16-hexaoxacyclooctadecane (18-crown-6) (Tokyo Chemical Industry. Co. Ltd.), acetone (Wako Pure Chemical Industries, Ltd.), potassium permanganate($KMnO_4$) (Wako Pure Chemical Industries, Ltd.), hydrochloric acid (HCl) (Wako Pure Chemical Industries, Ltd.), palladium carbon 10wt% (Wako Pure Chemical Industries, Ltd.), methanol (Wako Pure Chemical Industries, Ltd.), triethylamine (Et_3N) (Wako Pure Chemical Industries, Ltd.), *N*-methylpyrrolidone (NMP) (Tokyo Chemical Industry. Co. Ltd.)

2.2.2 *Synthesis of 2-benzyloxy-4-fluoronitrobenzene* ***1***

5-Fluoro-2-nitrophenol (10.0 g, 0.064 mol), benzyl bromide (8 mL, 0.064 mol), potassium carbonate (13.2 g, 0.094 mol) and *N*, *N*-dimethylformamide (DMF) (60 mL) were added into a flask. The mixture was heated at 90 ℃ overnight in an oil bath. The reaction mixture was poured into distilled water after it was cooled to room temperature. The precipitate was extracted with ethyl acetate (3×150 mL). The organic layer was washed with brine, dry over $MgSO_4$, and concentrated by rotary evaporator. The crude product was recrystallized from hexane to give yellow crystals. The yield was 11.4 g (73%). Melting point (*mp*): 53 ℃ (53-55 ℃ [36]).

2.2.3 *Synthesis of 4-(3-benzyloxy-4-nitrophenoxy)-3-methoxybenzaldehyde* ***2***

2-Benzyloxy-4-fluoronitro benzene (4.00 g, 0.026 mol), potassium carbonate (11.59 g, 0.083 mol), 18-crown-6 (0.40 g, 0.002 mol), vanillin (4.00 g, 0.026 mol), DMF (60 mL) were added into a flask. The mixture was heated for 12 h at 80 ℃. The reaction mixture was dissolved in dichloromethane, washed with distilled water. Then the organic layer was washed with sodium bicarbonate solution and brine three times, and was dried over $MgSO_4$, followed by concentration with rotary evaporator. The crude product was purified by column chromatography eluted with hexane and ethyl acetate = 3:2 and recrystallized to give yellow crystals. The yield was 6.09 g (80%). *mp*: 100 ℃. FT-IR (cm^{-1}): 2732 (CHO), 2824 (OCH_3), 1210 (C-O-C), 1278 (NO_2). ^{1}H NMR (DMSO-d_6, δ, ppm): 3.83 (s, 3H, -OCH_3), 5.29 (s, 2H, -CH_2), 6.50-6.54 (m, 1H, Ar-H), 7.03 (d, 1H, Ar-H, J = 2.41 Hz), 7.35-7.42 (m, 6H, Ar-H), 7.63-7.68 (m, 2H, Ar-H), 7.97-8.00 (d, 1H, Ar-H, J = 8.94 Hz), 10.03 (s, 1H, -CHO). ^{13}C NMR (DMSO-d_6, δ, ppm): 192.48, 162.04, 154.14, 147.74, 136.31, 134.97, 129.07, 128.61, 128.38, 127.88, 124.96, 122.60, 113.07, 108.32, 104.28, 71.19, 56.44. HRMS (ESI) calcd for C21H18NO6 $[M+H]^+$: 380.1129, found 380.1117.

2.2.4 *Synthesis of 4-(3-benzyloxy-4-nitrophenoxy)-3-methoxybenzoic acid* ***3***

4-(3-Benzyloxy-4-nitrophenoxy)-3-methoxybenzaldehyde (6.09 g, 0.016 mol), potassium permanganate (3.26 g, 0.021 mol) and acetone (150 mL) were added into a flask. The mixture was stirred for 4 h at room temperature. The reaction mixture was concentrated by rotary evaporator. Then it was dissolved in distilled water, and added dropwise with HCl to separate out brown solid. The precipitate was filtered and washed by distilled water to give brown powder. The yield was 5.80 g (91%). *mp*: 177 ℃. FT-IR (cm^{-1}): 3420 (COOH), 2953 (CHO), 2646 (OCH_3), 1692 (COOH), 1278 (NO_2). ^{1}H-NMR (DMSO-d_6, δ, ppm): 3.78 (s, 3H, -OCH_3), 5.28 (s, 2H, -CH_2), 6.47-6.50 (m, 1H, Ar-H), 6.98 (d, 1H, Ar-H, J = 2.41 Hz), 7.24-7.26 (d, 1H, Ar-H, J = 8.26 Hz), 7.33-7.42 (m, 5H, Ar-H), 7.63-7.69 (t, 2H, Ar-H, J = 17.20 Hz), 7.95-798 (d, 1H, Ar-H, J = 8.94 Hz). ^{13}C NMR (DMSO-d_6, δ, ppm): 162.41, 154.15, 151.37, 136.35, 129.61, 129.06, 128.61, 128.39, 127.90, 123.42, 122.43, 114.48, 107.96, 103.89, 71.16, 56.32. HRMS (ESI) calcd for C21H18NO7 $[M+H]^+$: 396.1078, found 396.1063.

2.2.5 *Synthesis of 4-(4-amino-3-hydroxy-phenoxy)-3-methoxy-benzoic acid hydrochloride* ***4***

4-(3-Benzyloxy-4-nitro-phenoxy)-3-methoxybenzoic acid (3.00 g), 10% palladium-charcoal catalyst (0.60 g, 10 wt%), HCl (4 mL), THF (50 mL) and methanol (50 mL) were added into a flask. The reaction mixture was stirred under hydrogen for 48 h at room temperature. The resulting mixture was filtered with celite® to remove the catalyst. The filtrate was concentrated by rotary evaporator. The crude product was recrystallized from sodium chloride solution to get purple powder. The yield was 2.4 g (81%). *mp*: 243 ℃ (dec.). FT-IR (cm^{-1}): 3420 (COOH), 3214 (OH), 2940 (NH_2), 2611 (OCH_3), 1684 (COOH), 1210 (C-O-C). ^{1}H NMR (DMSO-d_6, δ, ppm): 3.82-3.87 (s, 3H, -OCH_3), 6.44-6.46 (m, 1H, Ar-H), 6.59-6.62 (d, 1H, Ar-H, J = 2.41 Hz), 7.10-7.12 (d, 1H, Ar-H, J = 8.26 Hz), 7.32-7.34 (d, 1H, Ar-H, J = 8.60 Hz), 7.58-7.65 (m, 2H, Ar-H), 9.90 (s, 2H, -NH_2), 10.97 (s, 1H, -COOH).

^{13}C NMR (DMSO-d_6, δ, ppm): 167.23, 157.73, 152.26, 147.87, 128.47, 125.74, 123.39, 121.30, 114.45, 114.20, 108.16, 105.07, 56.33. HRMS (ESI) calcd for C14H14NO5 $[M+H]^+$: 276.0866, found 276.0892.

2.2.6 *Synthesis of poly(ether-o-hydroxy amide) (PEHA)* ***5***

4-(4-Amino-3-hydroxy-phenoxy)-3-methoxybenzoic acid hydrochloride (0.312 g, 0.001mol), diphenyl (2,3-dihydro-2-thioxo-3-benzoxazolyl) phosphonate (DBOP) (0.459 g, 0.0012 mol), Et_3N (0.28 mL, 0.002 mol), and dehydrated *N*-methyl-2-pyrrolidone (NMP, 3 mL) were added into a flask equipped with a condenser and a nitrogen inlet. DBOP was synthesized as reported in the literature [36]. The mixture was stirred for 24 h at room temperature under nitrogen. The reaction mixture was poured into methanol to precipitate the orange powder. The yield was 0.195 g (75%).

2.2.7 *Synthesis of poly(ether-benzoxazole) (PEBO)* ***6***

PEHA was dissolved in NMP (25 wt%) at room temperature. The solution was cast onto a glass plate. Then the casted solution was dried at 250℃ for 1 hour in a vacuum oven to form a PEBO film. The thickness of well-dried PEBO film was 45-64 μm.

2.2.8 *Characterization*

^{1}H- and ^{13}C-NMR spectra were obtained on a JEOL ALPHA300 instrument at 300 and 75 MHz, respectively. Deuterated dimethyl sulfoxide (DMSO-d_6) was used as a solvent with tetramethylsilane (TMS) as an internal standard. Fourier transform infrared spectra (FT-IR) were recorded with a JASCO FT-IR-4100 spectrophotometer. High-resolution mass spectra (HRMS) with an electrospray ionization system (ESI) were recorded on a micrOTOF-QII (Bruker Daltonics Inc.). Inherent viscosity of PEHA was measured using a Ubbelohde viscometer (Kusano Science Corp., Tokyo, Japan) with 0.1 g/dL in DMF at 18℃.

Differential scanning calorimetry (DSC) analysis was performed on a Rigaku DSC-8230 at heating rates of 10 ℃/min under a nitrogen atmosphere. Thermogravimetric analysis (TGA) was performed on a Rigaku Thermoplus EVOTG 8120 at heating rate of 10 ℃/min under flowing nitrogen. The mechanical properties were measured by a Universal Testing Machine (Strography VES05D).

2.3 Results and Discussion

2.3.1 Synthesis of PEBO

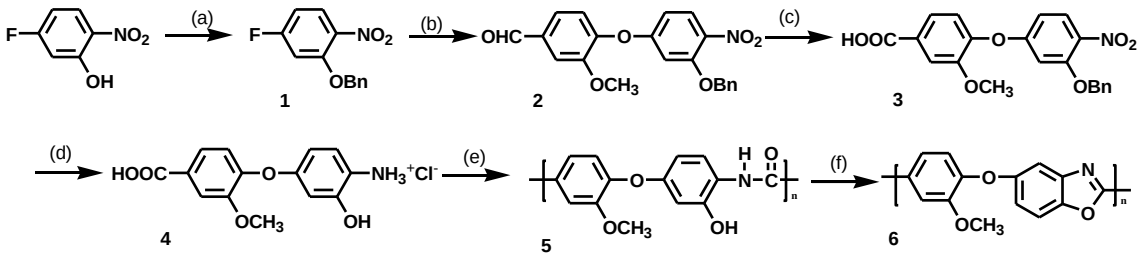

Scheme 2-1 Synthesis of PEBO. (a); BzBr, K_2CO_3, DMF, (b); Vanillin, K_2CO_3, 18-Crown-6, DMF, (c); $KMnO_4$, acetone, (d); Palladium 10% on carbon (Pd-C), HCl, (e); 2-Mercaptobenzoxazole, Et_3N, NMP, (f); Thermal treatment, NMP.

DBOP was synthesized by the reaction of 2-mercaptobenzoxazole with diphenyl chlorophosphate [36]. PEBO was synthesized by PEHA precursor **5**, which was prepared from monomer as shown in Scheme 2-1. The raw material 5-fluoro-2-nitrophenol was alkylated with benzylbromide in the presence of K_2CO_3 in DMF. Then alkylated 2-benzyloxy-4-fluoronitrobenzene **1** was reacted with vanillin to provide 4-(3-benzyloxy-4-nitrophenoxy)-3-methoxybenzaldehyde **2**. Subsequently compound **2** was oxidized to 4-(3-benzyloxy-4-nitrophenoxy)-3-methoxybenzoic acid **3** with $KMnO_4$. Pd-C was used for the amination to afford 4-(4-amino-3-hydroxyphenoxy)-3-methoxybenzoic acid hydrochloride **4** as PEHA precursor (monomer). The preparation of PEHA **5** was performed

according to previous literatures [38, 39]. PEHA **5** was converted to PEBO **6** by thermal ring closing reaction.

The chemical structure of novel bio-based monomer **4** was characterized by ^{1}H-NMR. All of the peaks in the ^{1}H-NMR spectrum were assigned as shown in Figure 2-1. Direct polycondensation of **4** using DBOP as a condensing agent successfully proceeded. Figure 2-2 shows ^{1}H-NMR spectrum of the PEHA **5**, where characteristic phenolic and amide protons were observed as well as methoxy and aromatic protons. The inherent viscosity of PEHA was 0.75 dL/g. After thermal cyclodehydration, no hydroxy and amide protons were observed as shown in Figure 2-3, confirming the transformation of PEHA to PEBO. Based on this result, the methoxy group was stable under the thermal cyclodehydration at 250 ℃ because the peak for methoxy group was still observed at 3.7-3.8 ppm in the ^{1}H NMR spectrum.

Figure 2-4 shows the FT-IR spectra of the monomer, PEHA, and thermal-treated PEHA (PEBO). For monomer, the characteristic C=O stretching band in carboxy group is observed at 1700 cm^{-1}. PEHA shows bands at 1650 (amide C=O stretch) and 1520 cm^{-1} (N-H bending) as expected. It is revealed that thermal treatment at 160 ℃ was not enough to dehydrate PEHA because of the presence of the residual amide and N-H peaks. After the thermal treatment at 250^{o}C, these peaks were negligible, and the bands characteristic for benzoxazole ring stretching clearly appeared at 1620, 1550, 1470, and 1060 cm^{-1}, suggesting that the ring closing reaction proceeded completely. Regardless of the thermal treatment, the characteristic peaks of ether were observed at 1270 (aromatic C-O-C asymmetric stretch) and 1030 cm^{-1} (aromatic C-O-C symmetric stretch). Therefore, the thermal cyclodehydration reaction of PEHA required 250 ℃ in order to convert PEHA to PEBO.

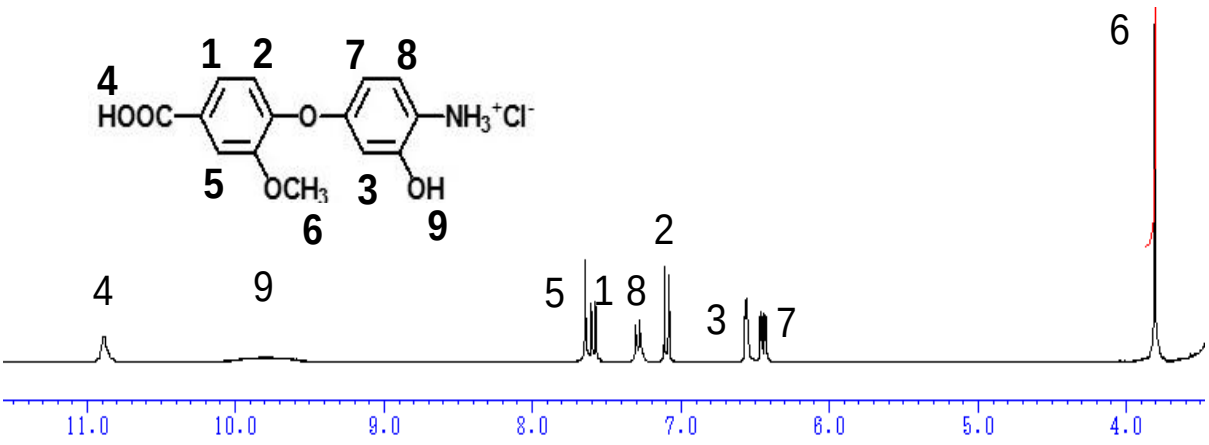

Figure 2-1 ^{1}H-NMR spectrum of PEHA precursor (monomer)

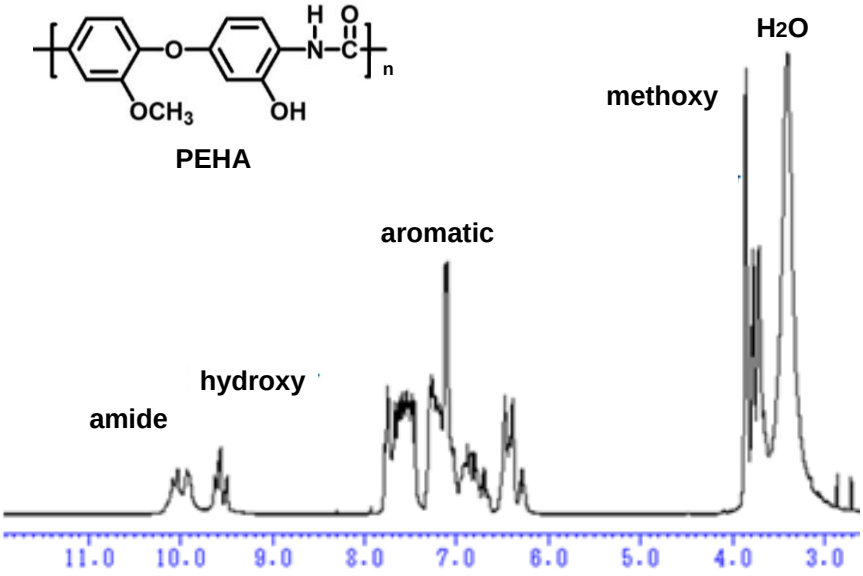

Figure 2-2 ^{1}H-NMR spectrum of PEHA

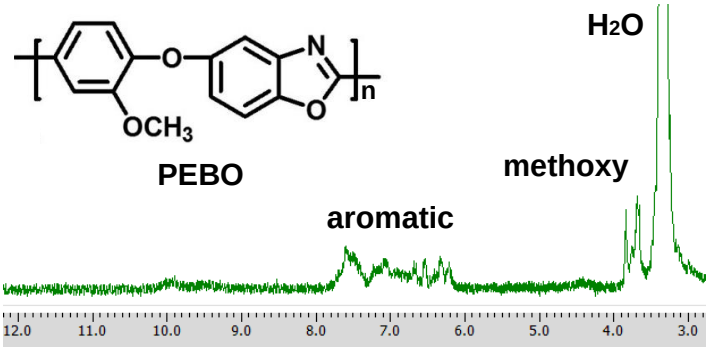

Figure 2-3 ^{1}H-NMR spectrum of PEBO

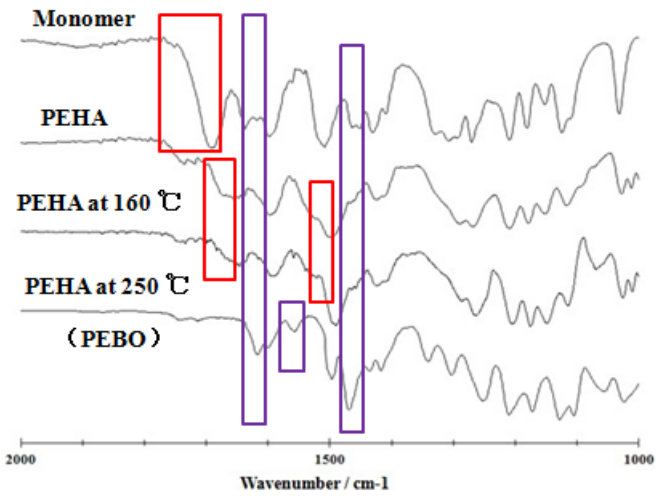

Figure 2-4 FT-IR spectra of the monomer, PEHA, and thermal-treated PEHA (PEBO)

2.3.2 Characterization of PEBO

The solubility of PEHA and PEBO in various solvents is summarized in Table 2-1. PEHA was soluble in NMP, DMF, DMSO and H_2SO_4, while PEBO was soluble in DMSO and H_2SO_4. Introduction of flexible ether moiety into the main chain, and the presence of methoxy group impeding the interchain packing improved solvent solubility compared with other PBO as reported in the literature [40]. Film quality of PEBO with changing curing temperature is summarized in Table 2-2. The film fabricated at 80 and 160 ℃ had poor film mechanical property, suggesting that the curing temperature was not enough to convert PEHA to PEBO as expected from FT-IR results. The film treated at 250 ℃ showed flexible and self-standing nature.

Table 2-1 Solvent solubility of PEHA and PEBO

Polymer	NMP	DMF	DMSO	H_2SO_4
PEHA	++	++	++	++
PEBO	−	−	+	++

++: Soluble at room temperature, +: partially soluble under heating (100 ℃), −: insoluble

Table 2-2 Film formation property of PEBO prepared at different temperature

Thermal condition (℃)	Thickness (μm)	Film property	FTIR spectra	Film color
80	64	Brittle	Amide group	Brown
160	58	Brittle	Amide group	Brown
250	62	Flexible (self-standing)	Benzoxazole group	Brown

Figure 2-5 shows the DSC curves of PEHA and PEBO (PEHA thermally treated at 250 ℃). An endotherm peak was observed between 230 and 260 ℃ (minimum point in the endothermic peak was 245 ℃) in the first scan of PEHA. On the other hand, there was no endothermic peak in DSC curve for the sample thermally treated at 250 ℃, PEBO as shown in Figure 2-5, indicating that the PEHA completed cyclodehydration reaction to PEBO. DSC curve also indicated that there was no obvious glass transition due to the rigid benzoxazole structure in PEBO. In addition, other thermal transitions such as crystalization and melting were not observed until 350 ℃.

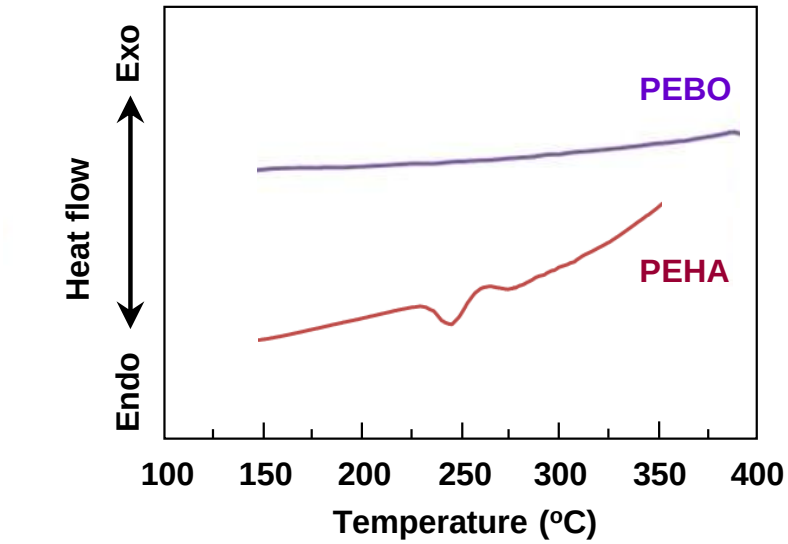

Figure 2-5 DSC curves of PEHA and PEBO

Figure 2-6 shows the TGA curves of PEHA and PEBO. PEHA precursor underwent two step weight losses with the increase of temperature. The first step from 240 to 300 ℃ was attributed to the conversion to cyclized polymers via dehydration (*e.g.*, PEBO). Therefore, this result is consistent with ^{1}H NMR, FTIR and DSC data, and it is reported that the ring closing reactions from PEHA to PEBO are carried out approximately at 250-300 ℃ [41, 42]. Theoretical weight loss induced by this cyclodehydration was estimated 7.0 wt% which was good agreement with the weight loss between 240 and 300 ℃ (*i.e.*, 7 wt%). The second step from 300 to 350 ℃ could be based on the decomposition of methoxy group. The theoretical percentage of methoxy group in the polymer was 12.1 wt% which was consistent with the weight loss between 240 and 300 ℃ (*i.e.*, 12 wt%). For both PEHA and PEBO, the thermal decomposition of polymer main chain gradually started at around 400 ℃. This degradation temperature is lower than those of other PEBO analogues. This is probably due to the presence of methoxy group in PEBO presented here.

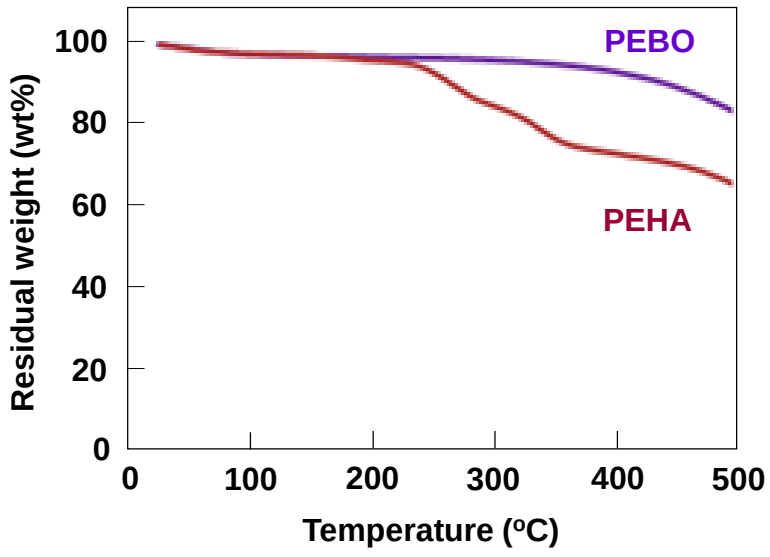

Figure 2-6 TGA curves of PEHA and PEBO

Figure 2-7 presents stress-strain curve of PEBO film, and the mechanical properties of PEBO together with those of other PBOs [42-45] and commercial engineering polymers are also summarized in Table 2-3. In this measurement, the author measured 2 samples (46 and 49 μm) to ensure the reproducibility. The result showed good reproducibility. The tensile strength and Young's modulus of the ether PBO films maintained 117 ± 6 MPa and 5.2 ± 0.7 GPa were observed. Presented PEBO showed better Young's modulus and tensile strength compared with other PEBOs [43, 44], and commercial engineering polymers.

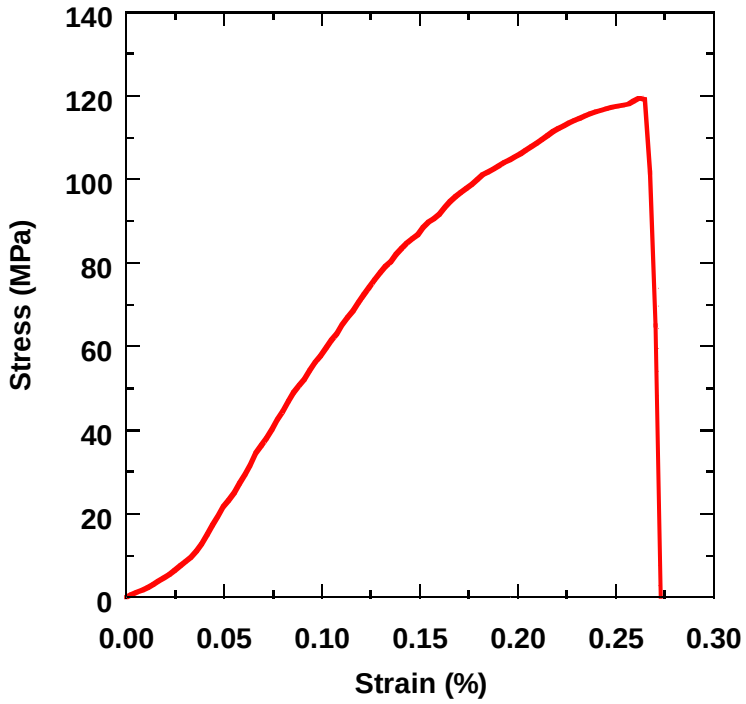

Figure 2-7 Stress-Strain curve of PEBO.

Table 2-3 Mechanical properties of PEBO compared with other polymers

Polymer	Thickness (μm)	Young's modulus (GPa)	Tensile Strength (MPa)	Reference
PEBO	49	5.2	117	This work
PBO [1]	10-15	11.7	332	[42]
PEBO [2]	30-80	1.8	64	[43]
PEBO [3]	50-60	1.9-2.4	35-105	[44]
PBO [4]	70-100	3	120	[45]
PI [5]	50	3.4	315	-
PEEK [6]	-	4.8	100	-

[1] PBO (PHA was synthesized with 3,3'- dihydroxybenzidine and isophthaloyl dichloride)

[2] PEBO (6F-PEBO)

[3] Cardo-type PEBO

[4] PBO (PBO was synthesized with 3,3'-dihydroxybenzidine, 3,3′-Dimethoxybenzidine, isophthaloyl dichloride, and glutaryl dichloride)

[5]from manufacture information of Kapton® H series

[6]from manufacture information of VICTREX® (aptiv®)

2.4 Conclusion

The novel biomass based PEBO was prepared via the direct polycondensation of the synthesized monomer derived from vanillin followed by thermal cyclodehydration. Synthesized PEHA precursor was soluble in common solvents such as NMP, DMF, DMSO and H_2SO_4, while PEBO was soluble in DMSO and H_2SO_4. Improved solubility is considered to be due to the introduction of flexible ether moiety into main chain and the presence of methoxy group derived from vanillin. A simple solvent casting of precursor PEHA and the subsequent thermal treatment at 250 ℃ afforded free-standing film exhibiting flexible and tough nature. DSC analysis showed that thermal cyclodehydration of PEHA into PEBO occurred in the range of 230- 260 ℃. Prepared PEBO did not show significant weight loss before 400 ℃, indicating moderate thermal stability. The tensile strength and Young's modulus of PEBO showed 117 MPa and 5.2 GPa, respectively. These values were higher than the other ether type PBO (PEBO) analogues and commercial engineering polymers.

2.5 References

1. C. Arnold, *J. Polym. Sci. Part D: Macromol. Rev*., **14,** 265 **(**1979).
2. J. F. Wolfe, "*Encyclopedia of Polymer Science and Engineering", Wiley Interscience, New York* (1985).
3. H. H. Yang, "*Aromatic High-Strength Fibers", Wiley: New York* (1989).
4. E. W. Choe and S. N. Kim, *Macromolecules,* **14,** 920 (1981).
5. T. Kitagawa, M. Ishitobi, and K. Yabuki, *J. Polym. Sci., Polym. Phys. Ed.,* **38**, 1605 (2000).
6. R. L. McGee, Y. H. So, S. J. Martin, C. F. Broomall, V. S Jeor, J. J. Curphy, E. J. Swedberg, and D. G. Wetters, *J. Polym. Sci., Part A: Polym. Chem.*, 35, 2157 (1997).
7. D. D. Feng, S. f. Wang, Q. X. Zhuang, P. Y. Guo, P. P. Wu, and Z. W. Han, *J. Mol. Struct*., **707**, 167 (2004).
8. T. Fukumaru, Y. Saegusa, T. Fujigaya, and N. Nakashima, *Macromolecules,* **47**, 2088 (2014).
9. K. Zhang, J. Liu, and H. Ishida, *Macromolecules,* **47**, 8674 (2014).
10. P. J. Walsh, X. Hu, P. Cunniff, and A. J. Lesser, *J. Appl. Polym. Sci*., **102**, 3517 (2006).
11. Y. Maruyama, Y. Oishi, M. Kakimoto, and Y. Imai, *Macromolecules,* **21**, 2305 (1988).
12. Y. Imai, K. Itoya, and M. Kakimoto, *Macromol. Chem. Phys.*, **201**, 2251 (2000).
13. Y. Oishi, A. Konno, J. Oravec, and K. Mori, *J. Photopolym. Sci. Technol*., **19,** 669 (2006).
14. G. L. Tullos, J. M. Powers, S. J. Jeskey, and L. J. Mathias, *Macromolecules,* **32**, 3598 (1999).
15. J. H. Chang, K. M. Park, S. M. Lee, and J. B Oh, *J. Polym. Sci., Part B.,* **38,** 2537 (2000).
16. S. L. Hsu, H. Chen, and S. Tsai, *J. Polym. Sci., Part A: Polym. Chem.,* **42**, 5990 (2004).
17. Y. Maruyama, Y. Oishi, M. Kakimoto, and Y. Imai, *Macromolecules,* **21,** 2305 (1988).

18. P. E. Cassidy, T. M. Aminabhavi, and J. M. Farley, *J. Macromol. Sci., Rev. Macromol. Chem. Phys.,* **C29**, 365 (1989).

19. J. G. Hilborn, J. W. Labadie, and J. L. Hedrick, *Macromolecules*, **23**, 2854 (1990).

20. J. L. Hedrick, J. Hilborn, T. D. Palmer, J. W. Labadie, and W. Volksen, *J. Polym. Sci., Part A: Polym. Chem.,* **28**, 2255 (1990).

21. W. D. Joseph, J. C. Abed, R. Mercier, J. E. McGrath, *Polymer,* **35**, 5046 (1994).

22. S. H. Hsiao and C. H. Yu, *Macromol. Chem. Phys.,* **199**, 1247 (1998).

23. S. H. Hsiao and C. H. Yu, *J. Polym. Sci., Part A: Polym. Chem.,* **37,** 2129 (1999).

24. K. H. Park, M. Kakimoto, and Y. Imai, *J. Polym. Sci., Part A: Polym. Chem.,* **36,** 1987 (1998).

25. G. Maglio, R. Palumbo, and M. Tortora, *J. Polym. Sci., Part A: Polym. Chem.,* **38,** 1172 (2000).

26. A. Llevot , E. Grau , S. Carlotti, S. Grelier, and H. Cramail, Macromol. Rapid Commun., **37**, 9 (2016).

27. J.D.P. Araujo, C.A. Grande, and A.E. Rodrigues, *Chem. Eng. Res. Des.*, **88**, 1024 (2010).

28. T. Koike, *Polym. Eng. Sci.*, **52**, 701 (2012).

29. C. Aouf, J. Lecomte, P. Villeneuve, E. Dubreucq, and H. Fulcrand, *Green Chem.*, **14**, 2328 (2012).

30. N.P.S. Chauhan, *Des. Monomers Polym.*, **15**, 587 (2012).

31. L. Mialon, A.G. Pemba, and S.A. Miller, *Green Chem.*, **12**, 1704 (2010).

32. L. Mialon, R. Vanderhenst, A.G. Pemba, and S.A. Miller, *Macromol Rapid Commun.*, **32**, 1386 (2011).

33. J.F. Stanzione III, J.M. Sadler, J.J. La Scala, K.H. Reno, and R.P. Wool, *Green Chem.*, **14**, 2346 (2012).

34. A.L. Holmberg, J.F. Stanzione, R.P. Wool, and T.H. Epps, *ACS Sust. Chem. Eng.*, **2**, 569 (2014).

35. A.S. Amarasekara, B. Wiredu, and A. Razzaq, *Green Chem*., **14**, 2395 (2012).

36. C.S. Hong, M. Jikei, and M. Kakimoto, *Polym. J.*, **35**, 859 (2003).

37. I. Bury, B Heinrich, C. Bourgogne, D. Guillon, and B. Donnio, *Chem. Eur. J.*, **12**, 8396 (2006).

38. M. Ueda, T. Morosumi, M. Kakuta, and R. Sato, *Polym. J.*, **22**, 733 (1990).

39. T. Hayakawa, T. Morishita, M. Okazaki, M. Ueda, K. Takeuchi, and M. Asai, *J. Polym. Sci., Part A: Polym. Chem.*, **38**, 3875 (2000).

40. Y. Imai, Y. Maeda, H. Takeuchi, K.H. Park, M. Kakimoto, and T. Kurosaki, *J. Polym. Sci., Part A: Polym. Chem.*, **40**, 2656 (2002).

41. C. S. Hong, M. Jikei, and M. Kakimoto, *Polym. J.*, **35**, 856 (2003).

42. J. H. Chang, K. M. Park, and I. C. Lee, *Polym. Bull.*, **44**, 63 (2000).

43. J. Lin and Y. M. Lee, *Macro. Phys.*, **207**, 1880 (2006).

44. S. H. Hsiao and M. H. He, *J, Polym, Sci.: Part A : Polym, Chem.*, **39**, 4014 (2001).

45. E. S. Yoo, A. J. Gavrin, R. J. Farris, and E.B. Coughlin, *High Perofrm. Polym*., **15**, 519 (2003).

Chapter 3 Synthesis and Characterization of Biobased Polyesters Derived From Vanillin-based Schiff Base and Cinnamic Acid Derivatives

Abstract

Renewable resources-based homo- and copolyesters were prepared from novel vanillin-based Schiff base and bio-based cinnamic acid derivatives by transesterification. Chemical structures of the Schiff base and resulting polyesters were confirmed by FT-IR, ^{1}H- and ^{13}C-NMR. Glass transition temperatures of polymers were determined by DSC and showed over 100^{o}C. Photoluminescent properties were investigated for the Schiff base and polyesters. For polymers, broader emission spectra were observed compared with monomers, which is probably originated from intramolecular charge transfer in each monomeric unit.

3.1 Introduction

Recently, biomass-based polymer materials derived from renewable resources such as plant and non-food products have received much attention because of the increasing price of petrochemical products, its depletion, and growing environmental concerns. The use of natural renewable resources derived from plant and non-food products would be one effective solution for this concern and beneficial in the development of novel environmentally-friendly polymer materials.

Vanillin, 4-hydroxy-3-methoxybenzaldehyde, is a renewable resources obtained from lignin. Vanillin has been used as a flavor in food and pharmaceutical industries because of its flavor property. In Chapter 2, vanillin-based poly (ether benzoxazole) was synthesized and characterized. *p*-Coumaric acid (*trans*-4-hydroxycinnamic acid CA) and ferulic acid (*trans*-4-hydroxy-3-methoxycinnamic acid, FA) are hydroxycinnamic acid (*E*-3-phenyl-2-propenoic acid) derivatives and obtained from rice bran and vegetables. Until now, many kinds of polymer materials using these natural renewable resources have been investigated and reported [1-10]. However, some of the materials are prepared with oil-based chemicals (*i.e.*, partial bio-based polymers). Therefore, development of wholly bio-based polymer materials has much attention and is important in a view of environmentally-friendly material design.

In this chapter, the synthesis and characterization of the all bio-based polyesters (*e.g.*, poly {3-[(3,4-dimethoxybenzylidene)amino]-4-hydroxy-5-methoxybenzoic acid} (DAHMBA), poly(CA), and poly(FA)) and their copolyesters (*e.g.*, poly(DAHMBA-*co*-CA)) and poly(DAHMBA-*co*-FA)) from a novel Schiff-based monomer which is derived from vanillin with *p*-coumaric acid and ferulic acid by transesterification are reported. Herein, the structure analyses of these bio-based polyesters and their functional properties with changing the different monomer ratio are discussed.

3.2 Experimental Section

3.2.1 Materials

Vanillin (Wako Pure Chemical Industries, Ltd.), potassium carbonate (Wako Pure Chemical Industries, Ltd.), acetic acid (Wako Pure Chemical Industries, Ltd.), nitric acid (Wako Pure Chemical Industries, Ltd.), hydrochloric acid (HCl) (Wako Pure Chemical Industries, Ltd.), ethanol (Wako Pure Chemical Industries, Ltd.), palladium carbon 10wt% (Wako Pure Chemical Industries, Ltd.), veratraldehyde (Wako Pure Chemical Industries, Ltd.), acetic anhydride (Wako Pure Chemical Industries, Ltd.), disodium hydrogen phosphate (Wako Pure Chemical Industries, Ltd.), *N*-methylpyrrolidone (NMP) (Tokyo Chemical Industry. Co. Ltd.), *N*,*N*-dimethylformamide (DMF) (Wako Pure Chemical Industries, Ltd.), methanol (Wako Pure Chemical Industries, Ltd.), *trans*-4-hydroxycinnamic acid (Wako Pure Chemical Industries, Ltd.), ferulic acid (Wako Pure Chemical Industries, Ltd.), DMSO-d_6 (Wako Pure Chemical Industries, Ltd.)

3.2.2 Synthesis of 4-hydroxy-3-methoxybenzoic acid (*vanillic acid*) ***1***

Vanillin (30 g, 0.2 mol), KOH (84 g, 1.5 mol) and H_2O (10 mL) were added into a round-bottom flask. The reaction mixture was stirred under air for 10 min at 180 ℃. After cooling to room temperature, 200 mL of water was added into flask and the solution was acidified to pH 3 with concentrated sulfuric acid. The resultant precipitate was collected with a filtration, and washed with water. The crude product was recrystallized from water to give a white powder. The yield was 25.6 g (76%), mp: 210 ℃ (208-209 ℃)[1].

3.2.3 Synthesis of 4-hydroxy-3-methoxy-5-nitrobenzoic acid (*5-nitrovanillic acid*) ***2*** [11]

To a solution of vanillic acid (20 g, 119 mmol) in acetic acid (200 mL) was added 60% nitric acid (9.7 mL, 126.4 mmol) dropwise. The reaction mixture was stirred at room temperature for 0.5 h, and then poured into ice-water. The resulting precipitate was filtered off, washed

with water, and dried under vacuum to give the product as a yellow powder. The yield was 11.28 g (44%), mp: 216-219 ℃ (216 ℃)[2].

3.2.4 *Synthesis of 3-amino-4-hydroxy-5-methoxybenzoic acid (5-aminovanillic acid) hydrochloride* ***3***

A mixture of 5-nitrovanillic acid (3 g, 139 mmol), palladium on carbon (10% Pd/C, 0.75 g, 25wt%) and 37% hydrochloric acid (3.2 mL, 141 mmol) in 200 mL ethanol was stirred at room temperature under H_2 overnight. After filtration, the solvent was evaporated to dryness affording the product as a white powder. The yield was 2.94 g (95.4%), mp: 232 ℃ (dec.) (215-257 ℃ (dec.))[3].

3.2.5 *Synthesis of 3-[(3,4-dimethoxybenzylidene)amino]-4-hydroxy-5-methoxybenzoic acid (5-veratrylideneaminovanillic acid) (DAHMBA)* ***4***

To a 100 mL flask were added 5-aminovanillic acid (1.1 g, 5 mmol), 3,4-dimethoxybenzaldehyde (veratraldehyde) (0.83 g, 0.5 mmol) and 25 mL ethanol. The mixture was stirred for 5 min at room temperature. Then, the precipitate was filtered off, washed with ethanol, and dried under vacuum to give the product as a yellow powder. The melting wasn't observed until 230°C before the pyrolysis. The yield was 1.18 g (71.3%). FT-IR (cm^{-1}): 1643 (C=O), 1590 (C=N), 1512 (aromatic ring). ^{1}H NMR (300 MHz, DMSO-d_6, δ, ppm, TMS): 3.83 (s, 3H, OMe) , 3.87 (s, 3H, OMe), 3.91 (s, 3H, OMe), 7.18 (d, 1H, ArH, J = 8.26 Hz), 7.40 (d, 1H, ArH, J = 1.72 Hz), 7.47 (d, 1H, ArH, J = 1.72 Hz), 7.57 (q, 1H, ArH, J = 1.72 and 2.41 Hz), 7.62 (d, 1H, ArH, J = 2.06 Hz), 9.85 (s, 1H, CNH). ^{13}C NMR (75 MHz, DMSO-d_6, δ, ppm, TMS): 56.0, 56.4, 56.7, 109.9, 111.8, 117.9, 120.9, 121.9, 126.7, 130.2, 144.6, 148.3, 149.7, 154.7, 167.0, 192.0. HRMS (ESI) calcd for C17H18NO6 [M+H]+ 332.1129, found 332.1127.

3.2.6 *Polymer Synthesis*

All homopolymers (poly (3,4,5-VAHMBA), poly (4-HCA), and poly (3,4-MHCA)) and copolymers (poly (3,4,5-VAHMBA-co-4-HCA) and poly (3,4,5-VAHMBA-co-3,4-MHCA) were synthesized according to the literature [12]. In a typical synthesis, poly(DAHMBA-*co*-CA) (50/50) was prepared by transesterification as follows. DAHMBA (2.1 mmol) and CA (2.1 mmol) were added into 5 mL of acetic anhydride containing disodium hydrogen phosphate and the mixture was stirred at 150 ℃ for 3 h. Then, the resultant was heated at 200 ℃ for 30 min under stirring, and then vacuumed for 15 min. The product was dissolved in chloroform and purified by reprecipitation with methanol. The final product was dried at 80 ℃ under vacuum for overnight. The other copolymers and homopolymers were synthesized with the similar manner for this copolymer.

Poly(DAHMBA): FT-IR (cm^{-1}): 1721 (C=O),1594 (C=N), 1510 (aromatic ring). ^{1}H NMR (300 MHz, $CDCl_3$-*d*, δ, ppm, TMS): 8.43 (azomethine proton), 6.85-7.70 (aromatic protons), 3.70-3.97 (methoxy protons).

Poly(DAHMBA-*co*-CA) (50/50): FT-IR (cm^{-1}): 1729 (C=O), 1599 (C=N), 1506 (aromatic ring). ^{1}H NMR (300 MHz, $CDCl_3$-*d*, δ, ppm, TMS): 8.43 (azomethine proton), 6.91-7.89 (aromatic protons and β-CH), 6.52-6.63 (α-CH), 3.88-4.09 (methoxy proton).

Poly(DAHMBA-*co*-FA) (50/50) : FT-IR (cm^{-1}): 1734 (C=O), 1600 (C=N), 1508 (aromatic ring). ^{1}H NMR (300 MHz, $CDCl_3$-*d*, δ, ppm, TMS): 8.43 (azomethine proton), 6.88-7.87 (aromatic protons and β-CH), 6.59-6.68 (α-CH), 3.88-4.08 (methoxy proton).

3.2.7 Characterization

^{1}H- and ^{13}C-NMR spectra were recorded on a JEOL ALPHA300 instrument at 300 and 75 MHz, respectively. Deuterated dimethyl sulfoxide (DMSO-d_6) or deuterated chloroform ($CDCl_3$) was used as a solvent with tetramethylsilane (TMS) as an internal standard. Fourier transform infrared spectra (FT-IR) were recorded with a JASCO FT-IR-4100 spectrophotometer. The number-average molecular weight (M_n), weight-average molecular weight (M_w), and polydispersity index (PDI; M_w/M_n) of each polymer were determined with a gel permeation chromatography equipped with a JASCO RI-2031 detector eluted with chloroform at a flow rate of 1.0 mL/min and calibrated by standard polystyrene samples. Ultraviolet–visible (UV–vis) absorption spectra of polymer solutions were obtained with a spectrometer (JASCO V-670). Photoluminescence (PL) measurements for monomers and polymers were performed on a spectrofluorometer (JASCO FP-6500). UV-vis and PL experiments were carried out for a 0.1 g/L of chloroform solution. Differential scanning calorimetry (DSC) analysis was performed on a Rigaku DSC-8230 at heating and cooling rates of 10 ℃/min under nitrogen atmosphere. The glass transition temperature, T_g was determined as the midpoint of the slope change on the curve. Thermogravimetric analysis (TGA) was performed on a Rigaku Thermoplus EVOTG 8120 at heating rate of 10 ℃/min under nitrogen atmosphere. High resolution mass spectometer (HRMS) with an electrospray ionization system (ESI) was recorded with a micrOTOF-QII-TND1.

3.3 Results and Discussion

3.3.1 Synthesis of DAHMBA

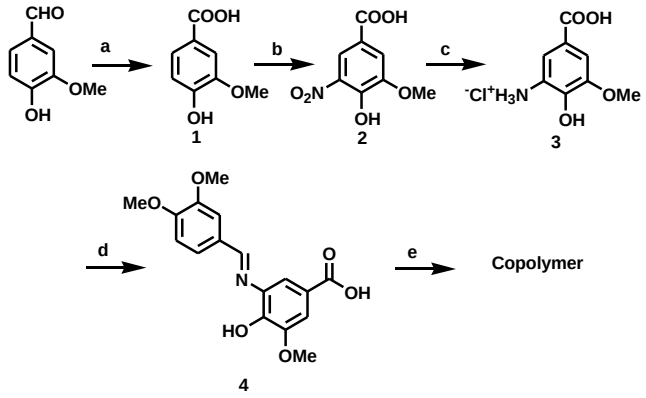

Scheme 3-1 Synthesis of 3-[(3,4-dimethoxybenzylidene)amino]-4-hydroxy-5-methoxybenzoic acid (DAHMBA) and homo- and copolymers with *p*-coumaric acid and ferulic acid. (a); KOH, (b); HNO_3, AcOH, (c); Palladium on carbon (Pd/C, 10% loading), ethanol, HCl, H_2, (d); Veratraldehyde, ethanol, (e); *p*-Coumaric acid or ferulic acid, acetic anhydride, disodium hydrogen phosphate.

3-[(3,4-Dimethoxybenzylidene)amino]-4-hydroxy-5-methoxybenzoic acid (DAHMBA) was synthesized by several reactions (Scheme 3-1). Firstly, vanillic acid **1** was prepared by the Cannizzaro reaction of vanillin. Nitration of vanillic acid was performed by H_2SO_4 according to the literature [11]. Then nitro group of nitro vanillic acid **2** was converted into amino group by Pd/C and H_2 gas and to give amino vanillic acid **3**. Finally, DAHMBA **4** was synthesized by the reaction of amino vanillic acid **3** and veratraldehyde. The chemical structure of novel Schiff-based monomer, DAHMBA **4** was characterized by ^{1}H- and ^{13}C-NMR as presented in Figures 3-1 and 3-2.

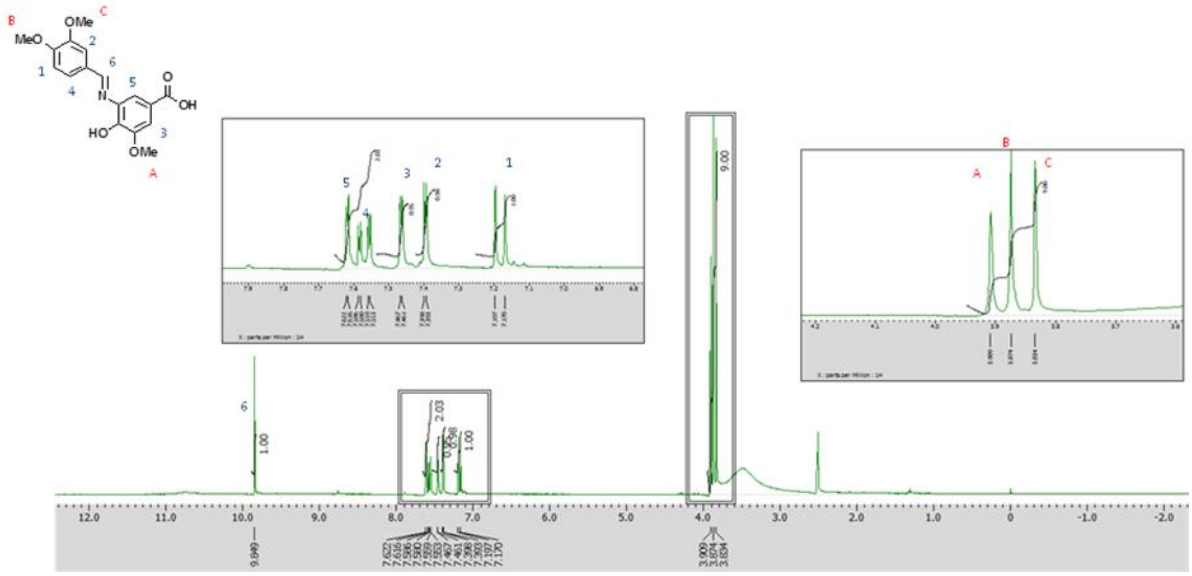

Figures 3-1 ^{1}H NMR spectrum of DAHMBA in chloroform at 300 MHz

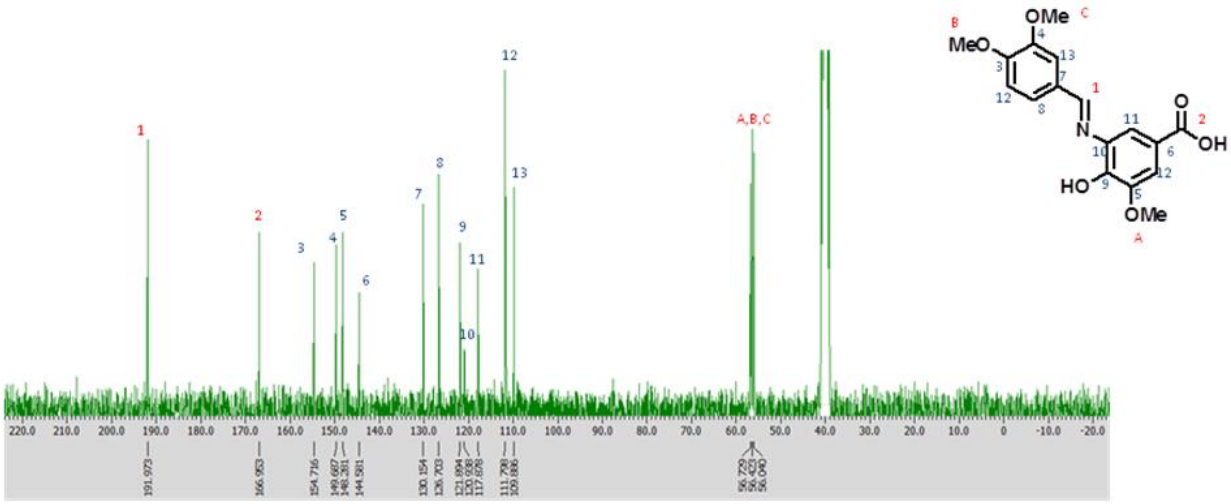

Figure 3-2 ^{13}C NMR spectrum of DAHMBA in chloroform at 75 MHz

Signal assignments for ^{1}H- and ^{13}C-NMR spectra of DAHMBA were carried out with the aid of ^{1}H-^{1}H COSY (correlated spectroscopy), ^{1}H-^{1}H NOESY (NOE correlated spectroscopy), HMQC (hetero-nuclear multiple quantum coherence spectroscopy), and HMBC (hetero-nuclear multiple-bond connectivity spectroscopy). The detail is as follows.

At first, judging from the chemical and multiplicity (Figure 3-1), the singlet signal around 9.1 ppm can be assigned to azomethine proton. It is also obvious that signals in the range of 7-8 ppm are originated from aromatic five types of protons, and the three set of singlet signals around 3.9 ppm are from three kinds of methoxy groups. According to ^{1}H-^{1}H COSY spectrum (Figure 3-3), pseudo doublet signal at 7.18 ppm is strongly correlated with the double doublet signal at 7.57 ppm, indicating that these signals can be assigned to aromatic protons adjacent each other in veratraldehyde moiety. For aromatic protons, the coupling constant, J_{ortho} is larger than J_{meta}, and J_{para} is less than 1 Hz. Therefore it is speculated that pseudo doublet at 7.18 is from proton 1 and double doublet at 7.57 ppm from proton 4 as shown in Figure 3-1. ^{1}H-^{1}H COSY spectrum also reveals that the signals at 7.62 and 7.47 ppm correlate weakly each other, indicating that these signals are from 5-aminovanillic acid moiety. Remaining pseudo doublet signal at 7.40 ppm should be from proton 2.

NOESY spectrum concerned with methoxy protons (Figure 3-4) ensures the above mentioned consideration and affords additional information. The signals of proton 1 (not proton 4) is correlated with methoxy proton signal (B) because of the steric vicinity. It is also found that proton 2 is in the vicinity of methoxy protons (C) as expected. Remaining the signals for methoxy protons (A) is correlated with that resonated at 7.47 ppm. From these results, the pseudo doublet signal at 7.47 ppm can be assigned to proton 3, and consequently that at 7.62 ppm (without correlation with methoxy protons) be to proton 5 as shown in Figure 3-1. All proton signals except of hydroxyl and carboxy protons (exchangeable protons) can be assigned.

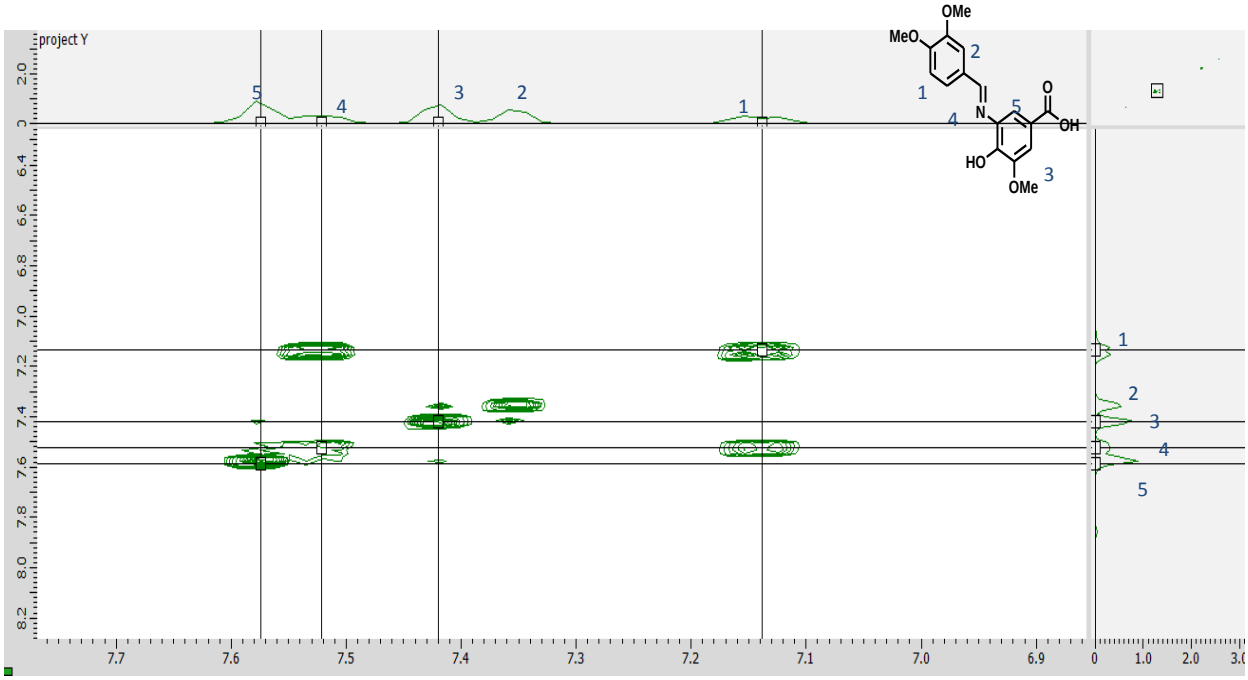

Figure 3-3 ^{1}H-^{1}H COSY spectrum of DAHMBA in chloroform at 300 MHz

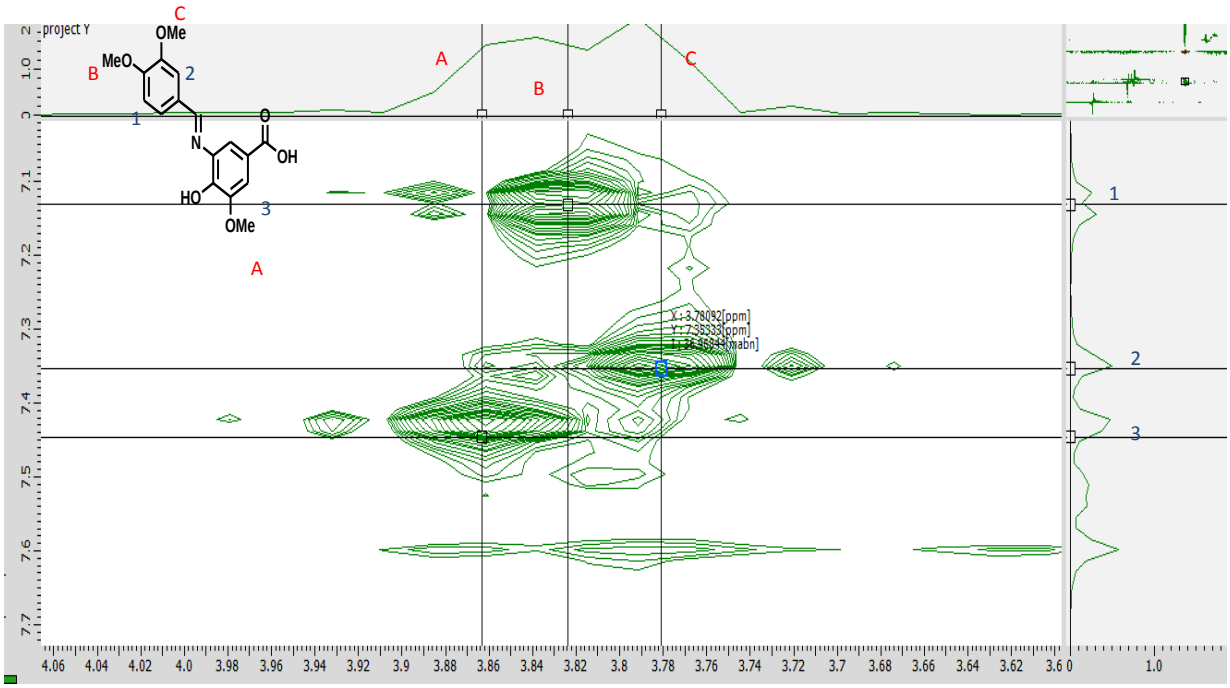

Figure 3-4 ^{1}H-^{1}H NOESY spectrum of DAHMBA in chloroform at 300 MHz

The signal assignments for ^{13}C-NMR spectrum are carried out as follows. Figure 3-5 shows entire ^{1}H-^{13}C HMQC spectrum of DAHMBA making it possible to assign uniquely ^{13}C

(quaternary carbons) signals since the assignments for ^{1}H- signal is completed. For example, Figure 3-6 shows expanded HMQC spectrum in aromatic region, and the signals from protonated carbons are assigned as shown in Figure 3-2. HMQC spectrum also demonstrates that there is no correlation peak in the lower magnetic field from 130 ppm, indicating that all signals in this region are originated from quaternary carbons.

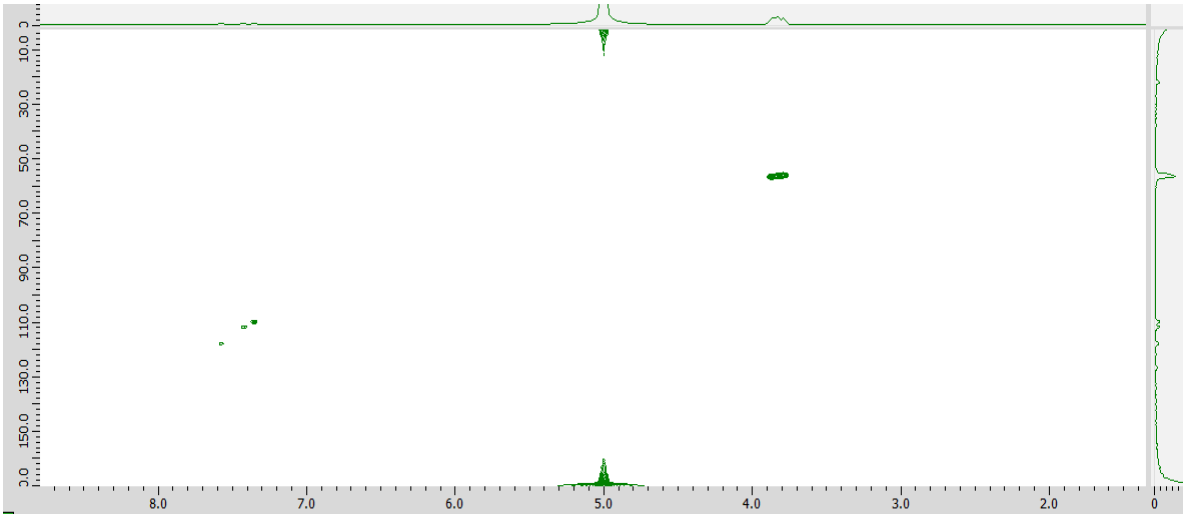

Figure 3-5 Entire ^{1}H-^{13}C HMQC (1) spectrum of DAHMBA in chloroform

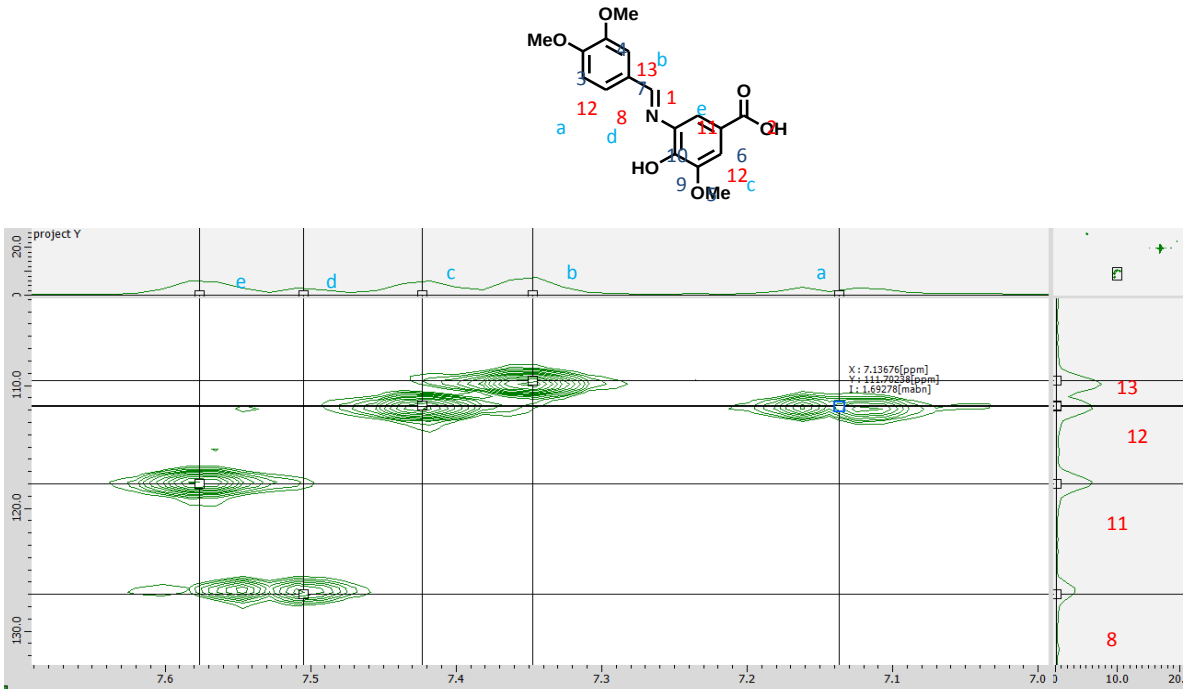

Figure 3-6 Expanded ^{1}H-^{13}C HMQC (2) spectrum of DAHMBA in chloroform

Finally the author describes how to assign the signals from the nine quaternary carbons without ambiguity with the aid of HMBC spectrum. Judging from chemical shift, two signals at lower magnetic field (192 and 167 ppm) can be assigned to azomethine and carbonyl carbons, and these assignments are consistent with HMBC results. Figure 3-7 shows partial HMBC spectrum confirming the correlation with methoxy protons. Three kinds of methoxy protons are apparently correlated with carbon signals around 150 ppm, which can be assigned to *ipso* carbons on which methoxy groups are substituted. Figure 3-8 focuses on the assignment of the signal at 144 ppm. From the correlation with two kinds of protons in 5-aminoferulic acid moiety, this signal is considered to be from carboxy substituted *ipso* carbon. Figure 3-9 shows the correlation of quaternary ^{13}C signal resonated at 130 ppm with azomethine proton (9.8 ppm) and proton at 5 position of veratrylidene group. This strongly suggests that the signal at 130 ppm is originated from *ipso* carbon with azomethine substituent. Remaining quaternary carbons are located on the aminovaniline moiety, amino and hydroxyl substituted carbons, which should appear at 121 and 122 ppm. Figure 3-10 shows the correlation of these carbons. Proton on the carbon adjacent to methoxy and carboxy groups is found to be correlated with ^{13}C-signal at 122 ppm, suggesting that this signal can be assigned to *ipso* carbon with hydroxy substituent. Consequently the signal at 121 ppm is to *ipso* carbon with amino substituent.

Signal assignments without ambiguity for all of ^{1}H- and ^{13}C- signals can be carried out, ensuring the successful synthesis of DAHMBA with high purity.

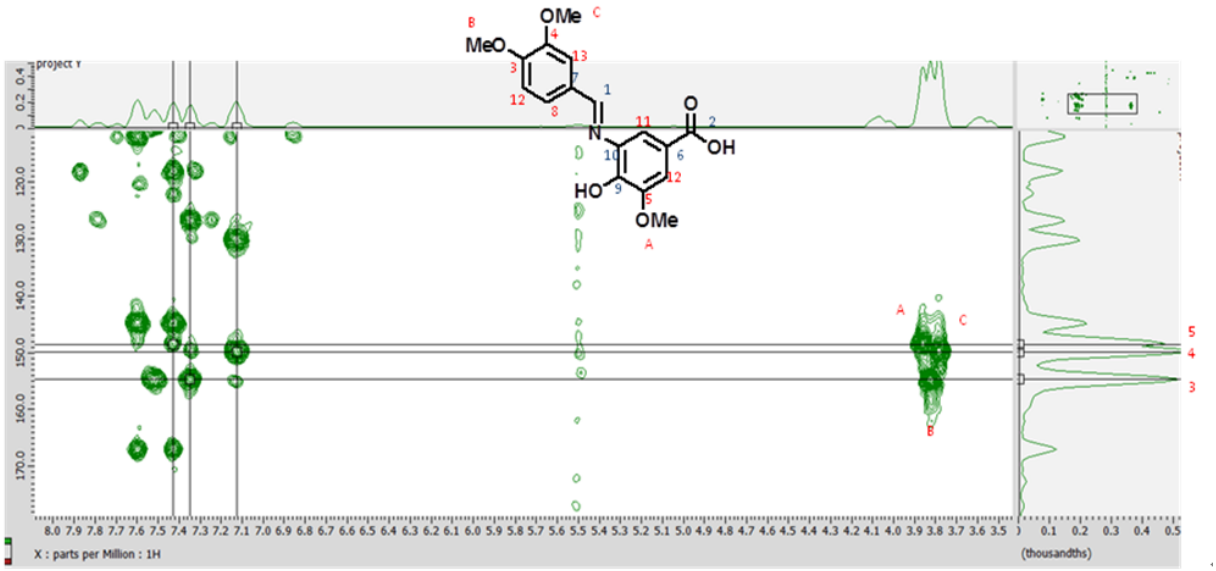

Figure 3-7 ^{1}H-^{13}C HMBC (1) spectrum of DAHMBA in chloroform

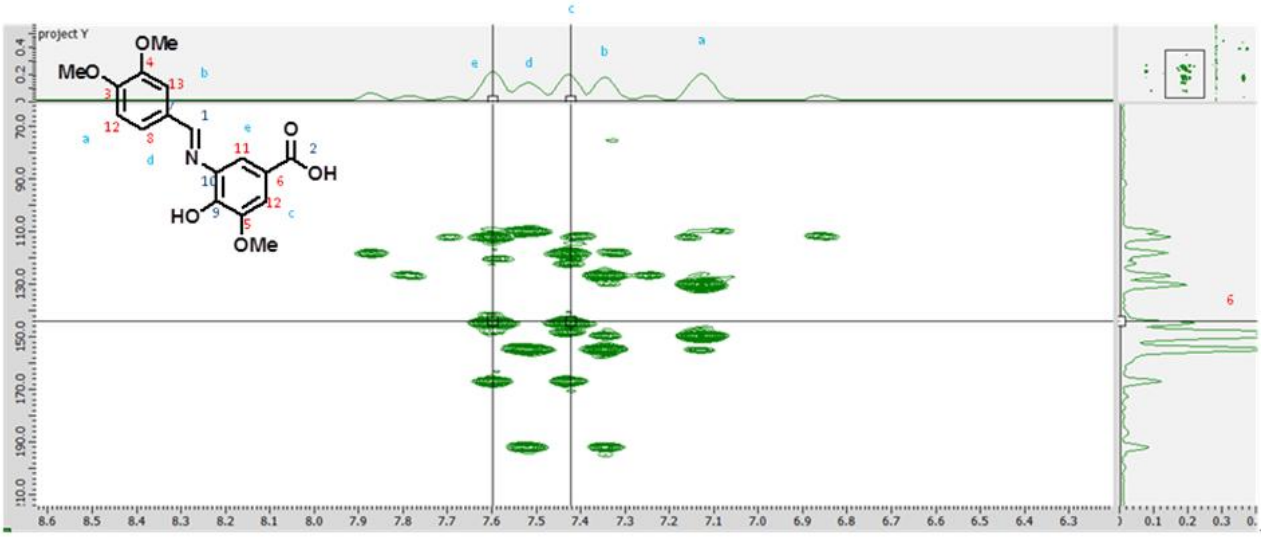

Figure 3-8 ^{1}H-^{13}C HMBC (2) spectrum of DAHMBA in chloroform

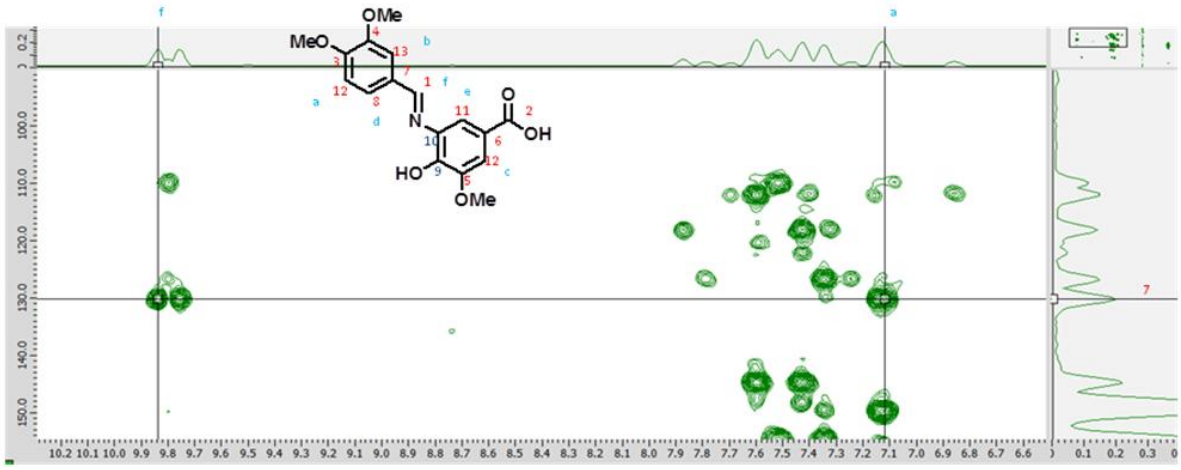

Figure 3-9 ^{1}H-^{13}C HMBC (3) spectrum of DAHMBA in chloroform

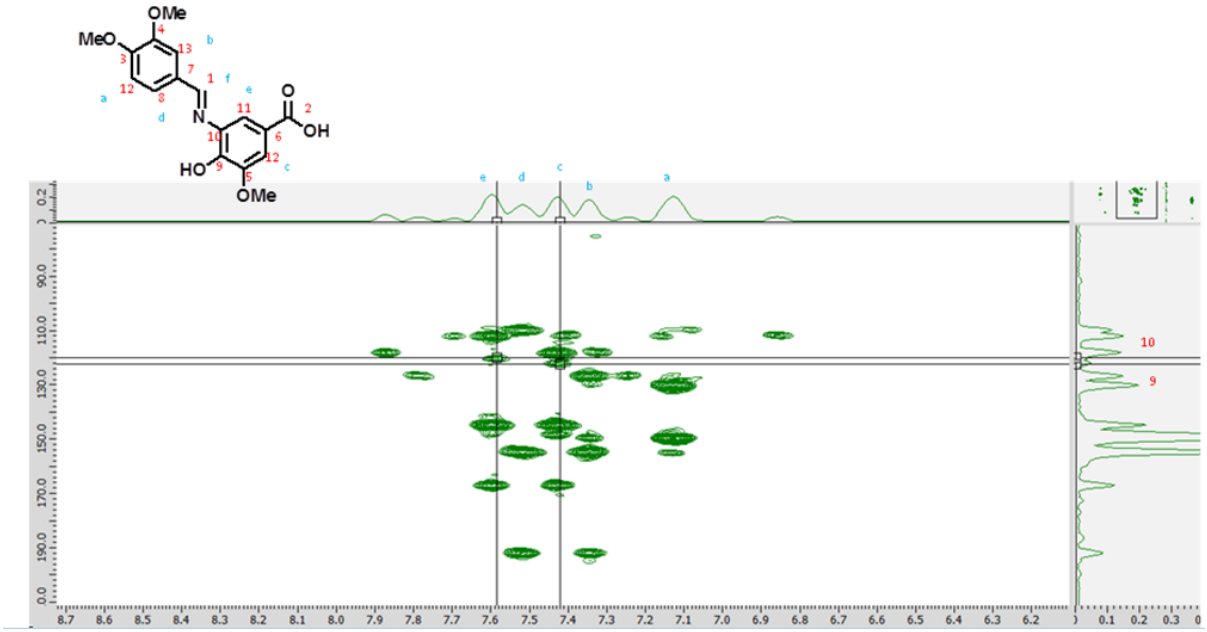

Figure 3-10 ^{1}H-^{13}C HMBC (4) spectrum of DAHMBA in chloroform

3.3.2 Polymer Synthesis

All homo- and copolymers were synthesized according to the literature [12]. Polymerization conditions and characteristics of polymers are listed on Tables 3-1 and 3-2. Actual composition of copolymer was determined by ^{1}H-NMR. As shown in Tables 3-1 and 3-2, the compositions of CA and FA in those copolymers were slightly higher than that in feed, indicating that reactivity of DAHMBA was slightly less than that of CA and FA. This is because that methoxy and bulky benzylidene amino groups near OH could restrain the polymerization due to their effect of steric hindrance compared with CA and FA.

Table 3-1 Polymerization conditions of poly(DAHMBA-*co*-CA)

Poly(DAHMBA-*co*-CA) (mol%)		DAHMBA	CA
in feed	in copolymer [(a)]	(mmol)	(mmol)
100/0	100/0	4.2	0
75/25	73/27	3.0	1.0
50/50	42/58	2.1	2.1
25/75	24/76	1.0	3.0
0/100	0/100	0	3.0

(a) Determined by ^{1}H-NMR measurement with $CDCl_3$ solvent

Table 3-2 Polymerization conditions of poly(DAHMBA-*co*-FA)

Poly(DAHMBA-*co*-FA) (mol%)		DAHMBA	FA
in feed	in copolymer [(a)]	(mmol)	(mmol)
100/0	100/0	4.2	0
75/25	65/35	3.0	1.0
50/50	47/53	2.1	2.1
25/75	22/78	1.0	3.0
0/100	0/100	0	2.1

(a) Determined by ^{1}H-NMR measurement with $CDCl_3$ solvent

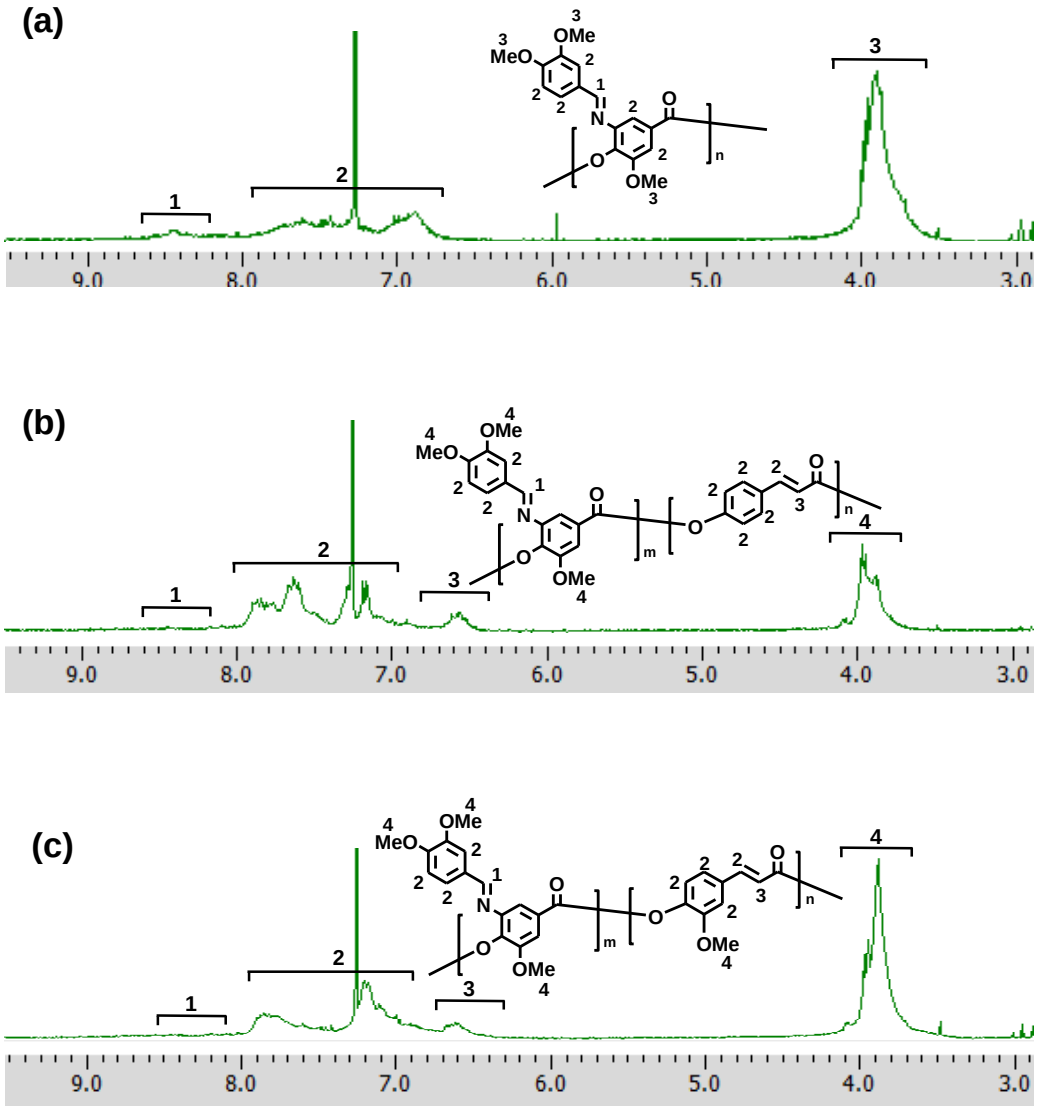

Figure 3-11 ^{1}H-NMR spectra of poly(DAHMBA)(a), poly(DAHMBA-*co*-CA)(b) and poly(DAHMBA-*co*-FA)(c) in chloroform at 300 MHz

The chemical structures of polymers were confirmed by ^{1}H-NMR in chloroform. Figure 3-11 represents ^{1}H-NMR spectra of poly(DAHMBA)(a), poly(DAHMBA-*co*-CA) and poly(DAHMBA-*co*-FA). In poly(DAHMBA)(a), the peak 1 (azomethine proton), peak 2 (aromatic protons) and the peak 4 (methoxy) were observed. In copolymers, the peak 1 (azomethine proton), the peak 2 (aromatic protons and β-CH), the peak 3 (α-CH) and the peak 4 (methoxy) were observed. Chemical compositions of copolymers were determined based on the signal integration.

Figures 3-12 present FT-IR spectra of poly(DAHMBA-*co*-CA)s. The terminal groups of homo- and copolymers (hydroxyl and carboxy groups) are observed near 3500 cm^{-1} in FT-IR. The spectra of homopolymer and copolymers show C=O stretching band near 1750 cm^{-1}, suggesting the conversion of carboxylic acid to phenyl ester. Figures 3-12 also represents FT-IR spectra of poly(DAHMBA-*co*- FA)s. Similar absorption pattern is observed.

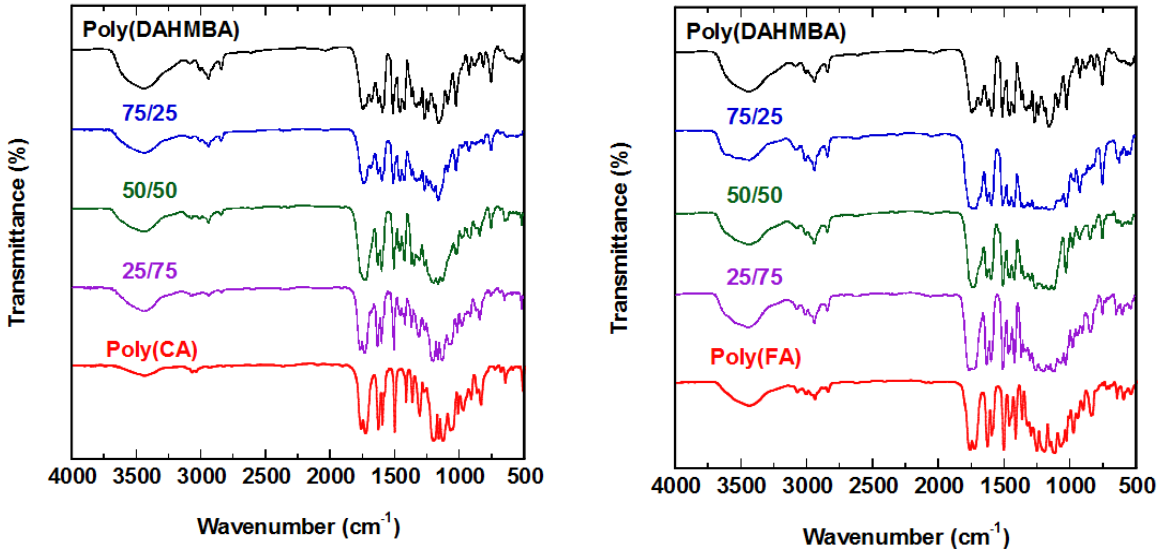

Figure 3-12 FT-IR spectra of poly(DAHMBA-*co*-CA)s(a) and poly(DAHMBA-*co*-FA)s (b)

Figure 3-13 shows DSC thermograms for poly(DAHMBA-*co*-CA)s, and thermal properties are summarized in Table 3-3. The glass transition temperatures (T_gs) of homopolymers were 108, and 120°C for poly(DAHMBA) and poly(CA), respectively. In addition, the melting of poly(CA) was observed at 188 ℃. Glass transition temperatures of both copolymers lie in the range of T_gs for the corresponding homopolymers.

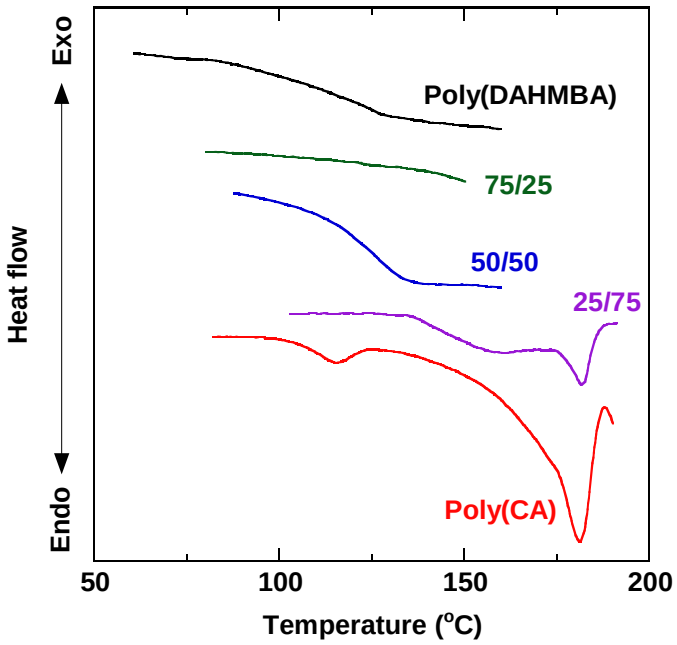

Figure 3-13 DSC curves of poly(DAHMBA-*co*-CA)s

Table 3-3 Thermal analysis date of poly(DAHMBA-*co*-CA)s

Polymer	Composition(mol%)	T_g (℃)	T_m (℃)
Poly (DAHMBA)	100/0	108	– [(a)]
Poly (DAHMBA-*co*-CA)	75/25	114	–
	50/50	119	–
	25/75	118	174
Poly (CA)	0/100	120	188

(a) not observed

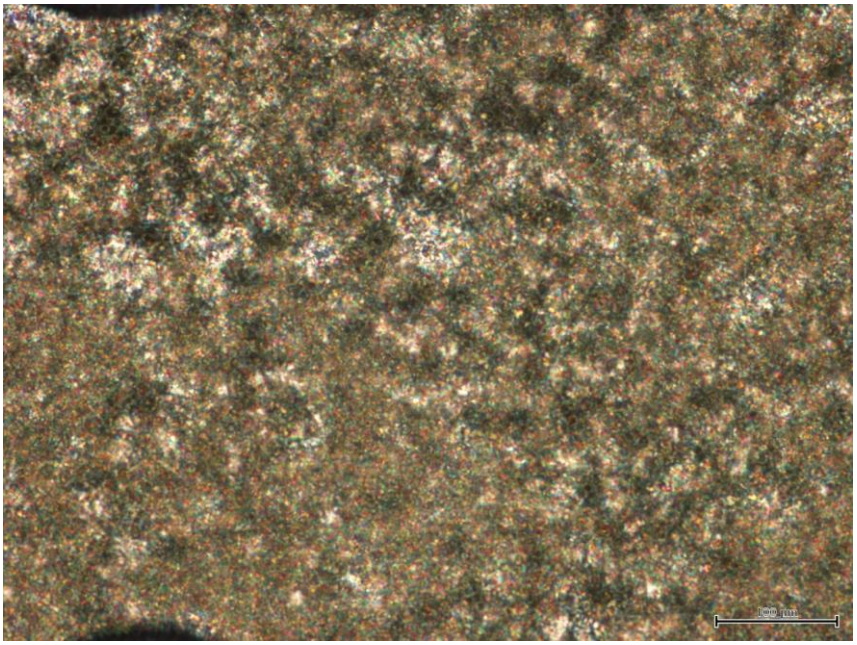

Figure 3-14 POM of poly(DAHMBA-*co*-CA) (25/75) at 215 ℃

The POM result of poly(DAHMBA-*co*-CA) (25/75) (Figure 3-14) indicated that poly(DAHMBA-*co*-CA) (25/75) showed liquid crystalline properties over their melting point at 215 and 210 ℃. Thermal properties of poly(DAHMBA-*co*-FA)s are also summarized in Figure 3-15 and Table 3-4. The glass transition temperatures (T_gs) of homopolymers were 108 and 112 ℃ for poly(DAHMBA) and poly(FA), respectively. The T_g of poly(FA) is in good agreement with the reported value of 113 ℃ [13]. The melting point is not observed in the DSC curves. Glass transition temperatures of both copolymers lie in the range of T_gs for the corresponding homopolymers. The POM results of poly(DAHMBA-*co*-FA)s indicated that these are not liquid crystalline polymers as predicted from DSC results.

Figure 3-16 shows the thermal gravimetric analysis (TGA) curves of DAHMBA monomer and homopolymer (a), poly(DAHMBA-*co*-CA)s (b), and poly(DAHMBA-*co*-FA)s (c). All polymers exhibit no weight loss until 250^{o}C.

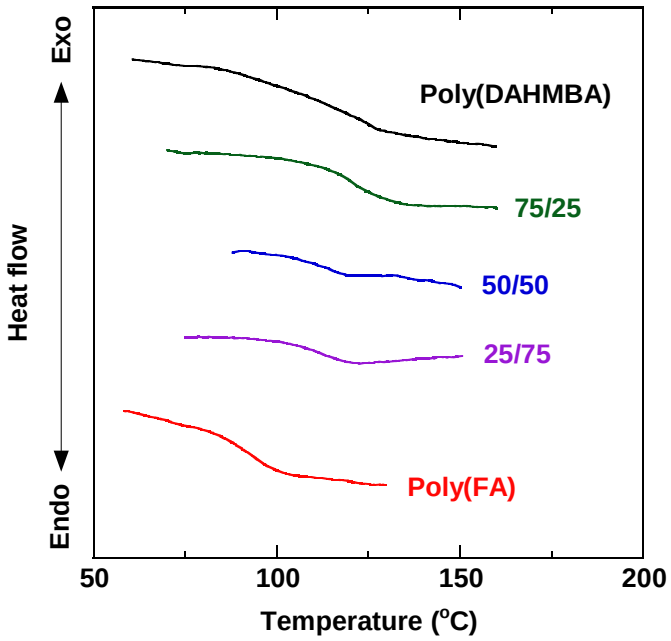

Figure 3-15 DSC curves of poly(DAHMBA-*co*-FA)s

Table 3-4 Thermal analysis data of poly(DAHMBA-*co*-FA)s

Polymer	Composition(mol%)	T_g (℃)	T_m (℃)
Poly(DAHMBA)	100/0	108	– [(a)]
Poly(DAHMBA-*co*-FA)	75/25	116	–
	50/50	116	–
	25/75	113	–
Poly (FA)	0/100	112	–

(a) not observed

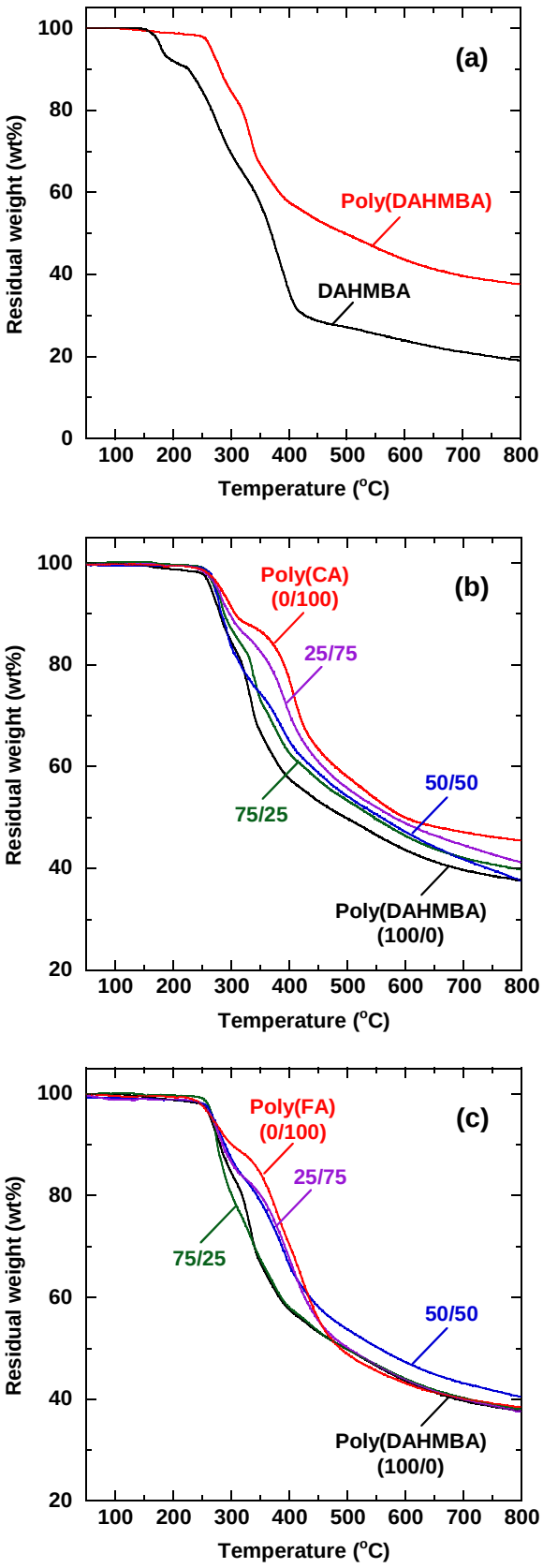

Figure 3-16 TGA curves of DAHMBA monomer and polymers. (a) DAHMBA and poly(DAHMBA), (b) poly(DAHMBA-*co*-CA)s, and (c) poly(DAHMBA-*co*-FA)s.

Table 3-5 Solvent solubility of poly(DAHMBA-*co*-CA)s

Sample	THF	DMAc	NMP	DMSO	$CHCl_3$	DMF	MeOH	EtOH	Acetone	H_2O	Toluene	Hexane
DAHMBA	+	+	+	+	−	+	+	+	+	−	−	−
CA	+	+	+	+	−	+	+	+	+	−	−	−
Poly (DAHMBA)	+	+	+	+	+	+	−	−	−	−	−	−
Poly (DAHMBA-*co*-CA) (75/25)	+	+	+	+	+	+	−	−	−	−	−	−
50/50	+	+	+	+	+	+	−	−	−	−	−	−
25/75	+	+	+	+	+	+	−	−	−	−	−	−
Poly (CA)	+	+	+	+	+	+	−	−	−	−	−	−

+: Soluble at room temperature, **−:** insoluble

Table 3-6 Solvent solubility of poly(DAHMBA-*co*-FA)s

Sample	THF	DMAc	NMP	DMSO	$CHCl_3$	DMF	MeOH	EtOH	Acetone	H_2O	Toluene	Hexane
DAHMBA	+	+	+	+	−	+	+	+	+	−	−	−
FA	+	+	+	+	−	+	+	+	+	−	−	−
Poly (DAHMBA)	+	+	+	+	+	+	−	−	−	−	−	−
Poly (DAHMBA-*co*-FA (75/25)	+	+	+	+	+	+	−	−	−	−	−	−
50/50	+	+	+	+	+	+	−	−	−	−	−	−
25/75	+	+	+	+	+	+	−	−	−	−	−	−
Poly (FA)	+	+	+	+	+	+	−	−	−	−	−	−

+: Soluble at room temperature, **−:** insoluble

The solubilities of synthesized polymers are summarized in Tables 3-5 and 3-6. The monomers, DAHMBA, CA, and FA are dissolved in various common solvents such as THF, DMAc, NMP, DMSO, DMF, methanol, ethanol, and acetone, while polymers are also dissolved in THF, DMAc, NMP, DMSO, $CHCl_3$, and DMF, however, they are insoluble to methanol, ethanol, and acetone which dissolved monomers, suggesting that the monomers are converted to form the polymers. In addition, the solubility of these copolymers is improved compared with copolymers prepared from CA and similar Schiff-based monomer without methoxy group [12]. This result suggests that the presence of methoxy group in the present work improved solubility due to the decrease of interchain interaction with the existence of methoxy groups unsymmetrical positions.

Molecular weights of synthesized polymers are summarized in Tables 3-7 and 3-8. The number average molecular weight of copolymers were 2100-4900 g/mol for poly(DAHMBA-*co*-CA) and poly(DAHMBA-*co*-FA) which were higher than that of poly(CA) and poly(FA). It is difficult to polymerize CA and FA to obtain high molecular weight of homopolymers because of poor solubility of higher molecular weight species [13]. The polydispercity of poly(DAHMBA-*co*-CA) and poly(DAHMBA-*co*-FA) is in the range of 1.1-2.1 and 1.6-2.1, respectively.

Table 3-7 Molecular weight of poly(DAHMBA-*co*-CA)

Poly(DAHMBA-*co*-CA) (mol%) [(a)]	M_n (g/mol)	M_w (g/mol)	PDI
100/0	4900	10000	2.1
75/25	2900	5000	1.7
50/50	3000	5700	1.9
25/75	2500	4900	1.9
0/100	2400	2500	1.1

(a) Composition in feed

Table 3-8 Molecular weight of poly(DAHMBA-*co*-FA)

Poly(DAHMBA-*co*-FA) (mol%) [1]	M_n (g/mol)	M_w (g/mol)	PDI
100/0	4900	10000	2.1
75/25	4200	6800	1.6
50/50	2700	5200	2.0
25/75	2100	3900	1.9
0/100	1100	2000	1.8

(a) Composition in feed

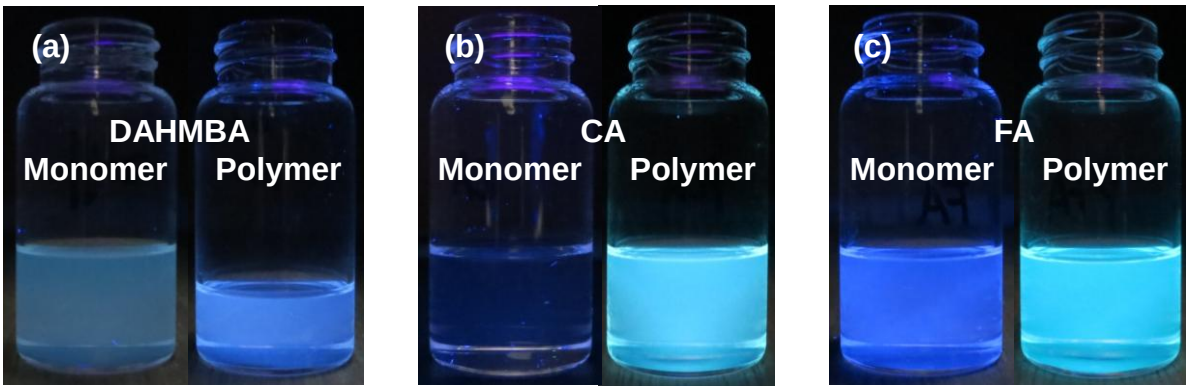

Figure 3-17 Photographs of chloroform solutions (0.1 g/L) irradiated by 365 nm UV light. Monomers and polymers of (a) DAHMBA, (b) CA, and (c) FA.

Table 3-9 Optical properties of monomers and polymers

Wave-Length	Monomer			Polymer		
	DAHMBA	CA	FA	DAHMBA	CA	FA
λ_{abs} (nm) [(a)]	277	311	321	300	311	326
λ_{em} (nm) [(a)]	383	382	387	424	468	471

Figure 3-18 shows photographs of the chloroform solution of monomers and their homopolymers irradiated by 365 nm UV light. DAHMBA showed blue photoluminescence as well as CA and FA, while similar 3-benzylideneamino-4-hydroxybenzoic acid without methoxy group shows weak visible photoluminescence [12].

The optical properties (ultra-visible absorption and photoluminescence) are summarized in Table 3-9. The wavelength of maximum absorbance (λ_{abs}) of poly(DAHMBA) and poly(FA) was red-shifted compared with each monomer, while that of poly(CA) was the same as that of monomer. Absorption spectra of copolymers exhibited superimposed absorptions of two homopolymers indicating that no specific interaction exists between two moieties in the ground state.

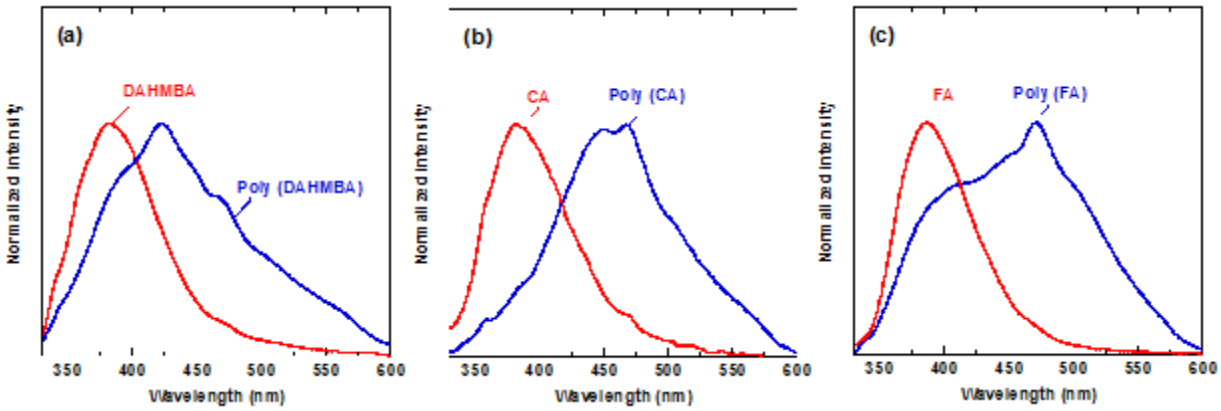

Figure 3-18 Photoluminescence spectra of monomers and polymers in chloroform (0.1 g/L). (a) DAHMBA, (b) CA, and (c) FA.

Figure 3-18 presents photoluminescence spectra for chloroform solution of monomers and homopolymers. As indicated in Table 3-9, polymerization induced the considerable red-shift of the wavelength of maximum emissions (λ_{em}) accompanied by broadening of emission. The solutions emit purple to pale blue fluorescence with large Stokes shifts. The largest Stokes shift was observed in the poly(FA) solution. Since all monomers involve donor-π-conjugation-acceptor systems, the intramolecular charge transfer state contributes to fluorescent properties. In polymers, excitons can interact with chromophores or dipoles in the vicinity leading to large Stokes shift and peak broadening.

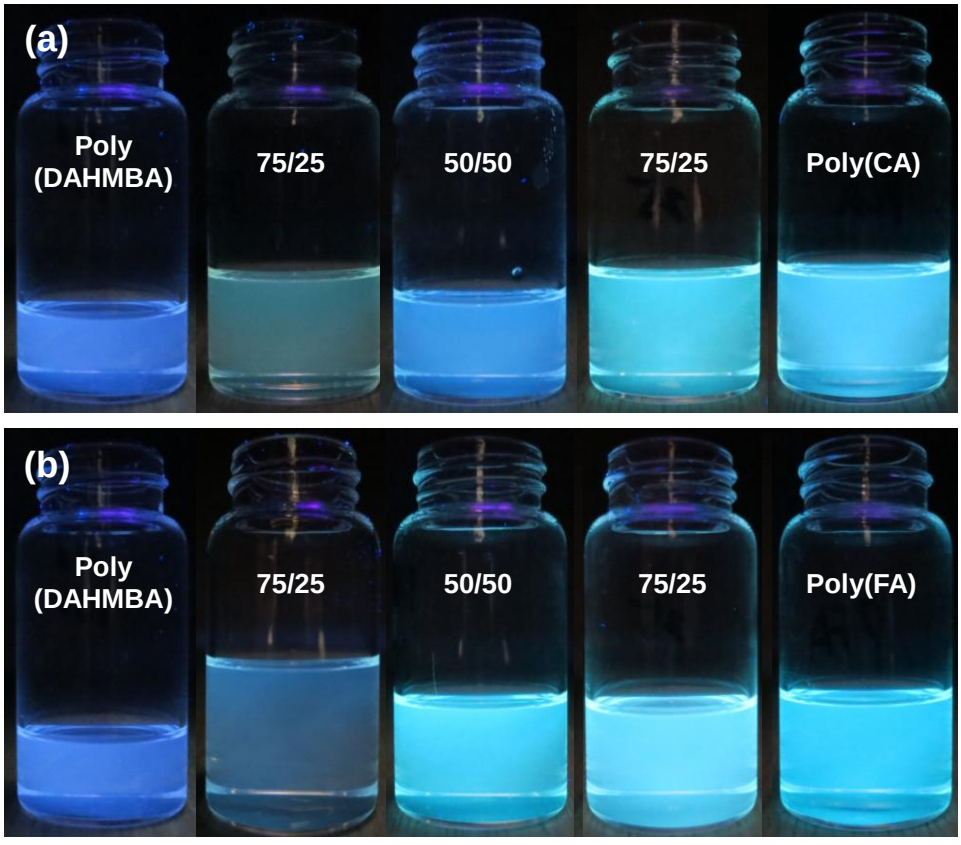

Figure 3-19 Photographs of chloroform solutions (0.1 g/L) irradiated by 365 nm UV light. (a) poly(DAHMBA-*co*-CA)s and (b) poly(DAHMBA-*co*-FA)s.

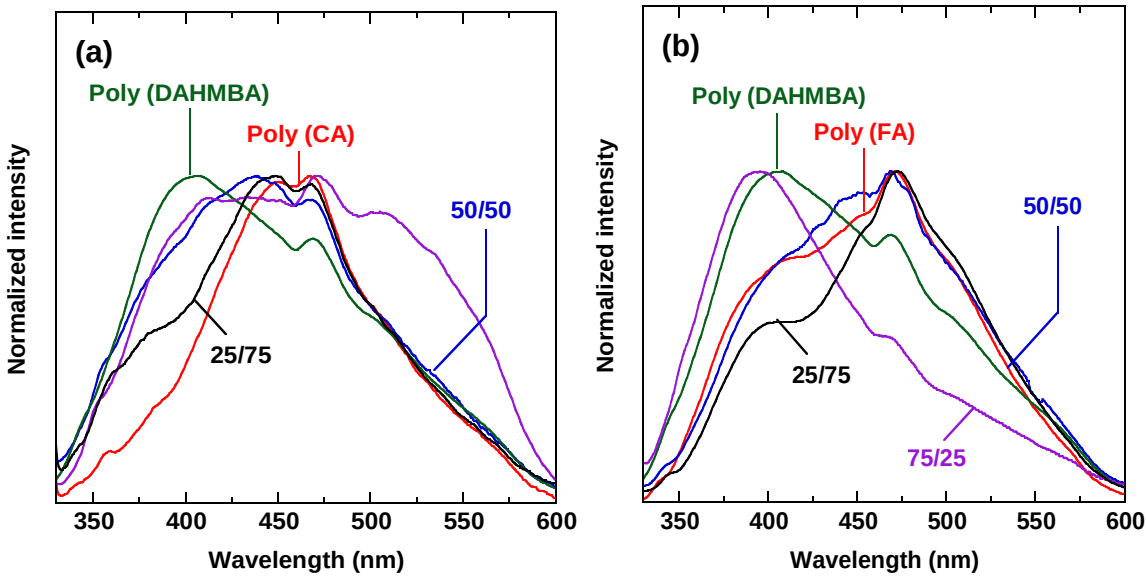

Figure 3-20 Photoluminescence spectra of poly(DAHMBA-*co*-CA) (a) and poly(DAHMBA-*co*-FA) (b) in chloroform (0.1 g/L).

Figure 3-19 shows photographs of poly(DAHMBA-*co*-CA) and poly(DAHMBA-*co*-FA) solutions irradiated by 365 nm UV light. Figure 3-20 represents photoluminescence spectra of poly(DAHMBA-*co*-CA) and poly(DAHMBA-*co*-FA) in chloroform. The photoluminescence spectrum of poly(DAHMBA-*co*-CA) appears as the superimposed emission from both homopolymers, while poly(DAHMBA-*co*-FA) shows almost the same spectrum as poly(FA) as expected from the solution color in Figure 3-19 over 50% of FA composition. Interestingly, the presence of methoxy group in FA moiety has a significant effect on emission behavior of copolymers.

3.4 Conclusion

The author synthesized novel Schiff base type monomer from vanillin and veratraldehyde, and homopolymerized the resulting monomer and copolymerized it with cinnamic acid derivatives (*i.e.,* CA and FA) via transesterification in order to produce wholly bio-based polymers. According to the molecular weight of homopolymers, the reactivity of this Schiff base type monomer was significantly higher than those of CA and FA. All monomers and polymers showed photoluminescence in chloroform solution under the irradiation of 365 nm UV light. Large Stokes shift was observed in the poly(FA) solution. The photoluminescence property of poly(DAHMBA-*co*-FA) was strongly affected by FA than DAHMBA. All polymers showed high glass transition temperature which was over 100 ℃. Thermal gravimetric analysis of polymers also showed a good thermal stability until 250 ℃. Hence, these bio-based polyesters can be expected as novel engineering thermoplastics.

3.5 References

1. M. Fache, B. Boutevin, and S. Caillol, *Eur. Polym. J.*, **68**, 488 (2015).
2. S. Kanehashi, T. Nagasawa, M. Kobayashi, S.L. Lee, M. Nakamura, S. Sato, M.F. Beristain, T. Ogawa, T. Miyakoshi, and K. Nagai, *J. Appl. Polym. Sci.*, **130**, 277 (2013).
3. T. Koike, *Polym. Eng. Sci.*, 52, 701 (2012).
4. C. Aouf, J. Lecomte, P. Villeneuve, E. Dubreucq, and H. Fulcrand, *Green Chem.*, **14**, 2328 (2012).
5. N.P.S. Chauhan, *Des. Monomers Polym.*, **15**, 587 (2012).
6. L. Mialon, A.G. Pemba, and S.A. Miller, *Green Chem.*, **12**, 1704 (2010).
7. T. Kaneko, T.H. Thi, D.J. Shi, and M. Akashi, *Nat. Mater.*, **5**, 966 (2006).
8. M. Chauzar, S. Tateyama, T. Ishikura, K. Matsumoto, D. Kaneko, K**.** Ebitani, and T**.** Kaneko**,** *Adv. Funct. Mater***.,** **22**, 3438 (2012).
9. D. Ishi, Koubunshi Ronbunshu, **70**, 449 (2013).
10. T.H. Thi, M. Matsusaki, D. Shi, T. Kaneko, and M. Akashi, *J. Biomater. Sci. Polym.*, **19**, 75 (2008).
11. L.E. Kiss, H.S. Ferreira, L. Torrão, M.J. Bonifácio, P.N. Palma, P. Soares-da-Silva, and D.A. Learmonth, *J. Med. Chem.*, **53**, 3396 (2010).
12. K. Kan, D. Kaneko, and T. Kaneko, *Polymers*, **3**, 861 (2011).
13. H.G. Elias and J.A. Palacios, *Makromol. Chem.*, 186, 1027 (1985).

Chapter 4 Radical Copolymerization of Ferulic Acid Derivatives with Ethylenic Monomers

Abstract

Bio-based ferulic acid (FA), (*E*)-3-(4-hydroxy-3-methoxyphenyl)prop-2-enoic acid was converted to 1,2-disubstituted ethylenic monomer (FA1) via methyl esterification followed by silylation with *tert*-butyldimethylsilyl chloride. Radical copolymerization of FA1 with styrene (St), methyl methacrylate (MMA), and 4-acetoxy-3-methoxystyrene (FA2) prepared from FA were carried out using azobisisobutyronitrile as an initiator at 80^{o}C. It is found that FA1 was copolymerized with St and FA2, but not with MMA. The formation of copolymers was confirmed by ^{1}H- and ^{13}C-NMR analyses. The reactivity ratios of FA1 and St estimated by the Fineman-Ross method are r_{FA1}=0.12 and r_{St}=2.46. In the case of the copolymerization of FA1 with FA2, the reactivity ratios, r_{FA1}=0.13 and r_{FA2}=2.66 were determined.

4.1 Introduction

Ferulic acid (FA), (*E*)-3-(4-hydroxy-3-methoxy-phenyl)prop-2-enoic acid is one of the bio-based sustainable chemicals, found in commelinid plants such as rice, wheat, oats, and pineapple. FA is the building block of lignocelluloses, and lignin. A variety of alkaline, acid, and enzymatic methods for the extraction and isolation of FA have been reported in the literature.[1-6] As recently reviewed, FA has been widely applied in biomedical, pharmaceutical, food, cosmetic and other industries.[7] It is also of interest to prepare polymeric materials using bio-based FA as a starting material from the view point of sustainable development.

FA is a multi-functional chemical possessing hydroxyl, and carboxy groups. Using these functional groups, PET mimics polyester [8], poly(ester-alkenamer)s via an acyclic diene metathesis reaction [9], poly(ester-urethane)s [10], aliphatic–aromatic copolyesters [11] have been prepared. Since FA has a double bond conjugated with carbonyl and aryl groups, it is also regarded as one of the 1,2-disubstituted ethylenes. In the case of vinyl polymerization, hydroxyl and carboxy groups are not consumed in the polymerization reaction, and remain in the side chains leading to the other type of functional polymers. Radical polymerization of FA and its derivative or copolymerization with comonomers is an easy way to achieve bio-based polymers. It is generally believed that 1,2-disubstituted ethylenic monomers are not radically homopolymerized due to the steric hindrance except for N-alkyl or phenyl maleimides [12], and fumarates with bulky ester alkyl groups [13]. Meanwhile, 1,2-disubstituted monomers such as cinnamate and maleic anhydride can be copolymerized with conventional monomers such as styrene, and methyl methacrylate. FA is considered as an analogue of cinnamic acid, where phenolic hydroxy and methoxy groups are additional functional groups to cinnamic acid.

In this chapter, copolymerization behaviors of FA modified monomer with styrene, methyl methacrylate and styrene derivative resulting from the decarbonation of FA [14] are

investigated. In order to design novel renewable polymeric materials, it is of importance to understand the basic characteristics of FA derivatives in a radical polymerization.

4.2 Experimental Section

4.2.1 Materials

Ferulic acid (Wako Pure Chemical Industries, Ltd.), sulfuric acid (Wako Pure Chemical Industries, Ltd.), methanol (Wako Pure Chemical Industries, Ltd.), *tert*-butyldimethylsiyl chloride (Wako Pure Chemical Industries, Ltd.), imidazole (Wako Pure Chemical Industries, Ltd.), *N*,*N*-dimethylformamide (DMF) (Wako Pure Chemical Industries, Ltd.), styrene (Wako Pure Chemical Industries, Ltd.), azobis(isobutyronitrile) (AIBN) (Tokyo Chemical Industry. Co. Ltd.), triethylamine (Wako Pure Chemical Industries, Ltd.), acetic anhydride (Wako Pure Chemical Industries, Ltd.), toluene (Wako Pure Chemical Industries, Ltd.), methyl methacrylate (MMA) (Wako Pure Chemical Industries, Ltd.)

4.2.2 Synthesis of trans-4-hydroxy-3-methoxy cinnamic acid methyl ester

To a 200-mL two-necked round bottom flask equipped with a condenser, and a magnetic stirrer were added FA (3.0 g, 0.015 mol) and methanol (80 mL). After the addition of ten drops of sulfuric acid, the solution was refluxed for 24 h. After the evaporation of methanol, the residual yellow oil was dissolved in ethyl acetate followed by washed with sodium bicarbonate solution and brine. After drying with magnesium sulfate, the solvent was removed, and the resulting yellow oil was dried in vacuo (3.13 g, 99%).

4.2.3 *Synthesis of trans-4-tert-butyldimethlysiloxy-3-methoxy cinnamic acid methyl ester (FA1)*

To a 100-mL two-necked round bottom flask equipped with a magnetic stirrer and a dropping funnel was added *trans*-4-hydroxy-3-methoxy cinnamic acid methyl ester (3.13 g, 0.015 mol), imidazole (11.3 g, 0.045 mol), and 20 mL of dehydrated *N*, *N*-dimethylformamide. *tert*-butyldimethylsilyl chloride (7.56 g, 0.03 mol) was added dropwise at room temperature, and the reaction mixture was stirred for 4h. After the addition of 50 mL of water, the resulting solution was extracted with ethyl acetate (20 mL x 3). The organic layer was washed with brine, and the solvents were evaporated. The crude product was purified with column chromatography (silica, hexane / ethyl acetate =5 / 1). Recrystallization from ethanol afforded a colorless crystal (3.78 g, 81%, m.p.: 65^{o}C) [15]. ^{1}H NMR (300 MHz, $CDCl_3$), δ (ppm) from TMS: 7.60 (d, 1H, *J*=16.2 Hz), 7.00(m, 2H), 6.84 (d, 1H, *J*=8.7 Hz), 6.28 (d, 1H, *J*=16.2 Hz), 3.80 (s, 3H), 3.76 (s, 3H), 0.97 (s, 9H), 0.15 (s, 6H). ^{13}C NMR (75 MHz, $CDCl_3$) δ (ppm) from TMS: 167.57, 151.07, 147.42, 144.86, 128.14, 122.12, 120.97, 115.37, 110.71, 56.27, 51.46, 25.57, 18.37, -4.70.

4.2.4 *Synthesis of 4-acetoxy-3-methoxystyrene (FA2)*

To a 200-mL two-necked round bottom flask equipped with a magnetic stirrer and a condenser was added FA (5.0 g, 0.026 mol), triethylamine (2.45 mL, 0.026 mol), and 100 mL of toluene. The resulting dispersion was refluxed for 7 h. After confirming decarbonation, acetic anhydride (3 mL, 0.027 mol) and trimethylamine (3 mL, 0.029 mol) were added. After stirring for 5 h, the reaction mixture was cooled to room temperature, washed with sodium bicarbonate solution and brine three times, successively. The crude product was purified with column chromatography (silica, hexane / ethyl acetate =3 / 1). Evaporation of the solvents afforded reddish oil (4.42 g, 81%). ^{1}H NMR (300 MHz, $CDCl_3$), δ (ppm) from

TMS: 6.98 (m, 3H), 5.66 (dd, 1H, *J*=15.5 Hz, 9.5 Hz), 5.67 (dd, 1H, *J*=15.5 Hz, 3.0 Hz), 5.23 (dd, 1H, *J*=9.5Hz, 3Hz), 3.81 (s, 3H), 2.28 (s, 3H).

4.2.5 *General procedure of copolymerization of FA1*

To a glass ampule equipped with a magnetic stirrer, and a three-way stop-cock were charged with the mixture of FA1 and another monomer (total amount; 6.9 mmol), and AIBN (2 mol%). After four freeze-pump-thaw cycles, the reaction tube was heated at 80^{o}C under nitrogen atmosphere. The reaction mixture was poured into methanol to precipitate the product. Reprecipitation procedure was carried out twice, and the product was dried overnight in vacuo.

4.2.6 *Characterization*

^{1}H- and ^{13}C-NMR spectra were obtained on a JEOL ALPHA300 instrument at 300 and 75 MHz, respectively. Deuterated chloroform ($CDCl_3$) was used as a solvent with tetramethylsilane (TMS) as an internal standard. Molecular weight and its distribution were estimated with gel permeation chromatography equipped with JASCO 880-PU pump, a column packed with styrene-divinylbenzene gel beads [16], and a JASCO UV-970 detector. Chloroform was used as an eluent, and the molecular weitght was calibrated using polystyrene standards.

4.3 Results and Discussion

4.3.1 *Monomer Synthesis*

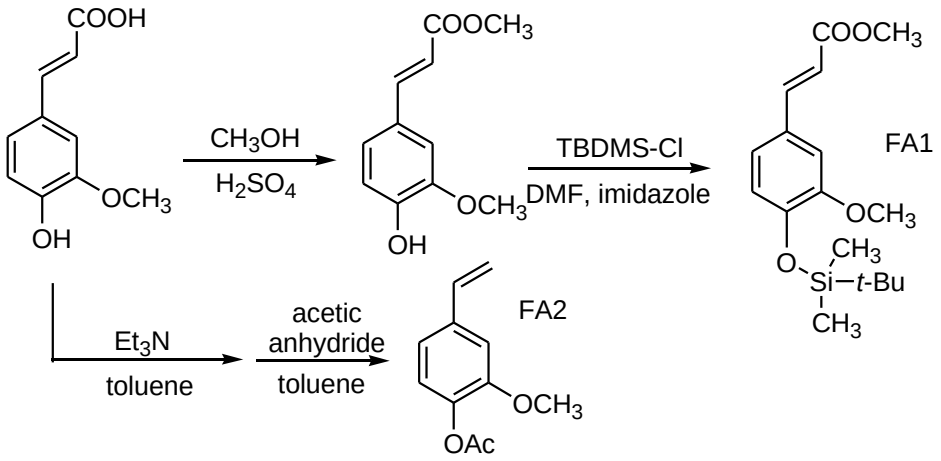

Scheme 4-1 Synthesis of monomers from ferulic acid (FA)

As shown in introduction, FA possesses phenolic hydroxyl group. In general radical polymerizations, hydrogen abstraction reaction of a propagating radical from hydroxyl group in a phenol derivative efficiently occurs, and the resulting radical is subject to the combination reaction with the other radical species (degradative chain transfer).[17] Consequently phenol acts as an inhibitor in radical polymerizations. Preliminary study revealed that solubility of FA derivative where hydroxyl group is protected by acetyl group is still not sufficient to be copolymerized with styrene in a bulk or a high concentrated solution. In the molecular design in this study, hydroxy group in FA is protected by *tert*-butyldimethylsilyl group, and carboxy group is converted to methyl ester in order to improve the solubility.

Designed monomer (FA1) was synthesized via two step processes, *i.e.* methyl esterification and subsequent silylation as shown in Scheme 4-1. Both reactions proceeded in over 80% yields, and in high purities. In ^{1}H-NMR spectrum of resulting FA1, two types of methoxy signals appear at 3.76 and 3.80 ppm. Two kinds of protons in the protecting silyl group show singlet signals at 0.15 and 0.97 ppm. All other signals can be assigned to

confirm that the desired molecule was obtained. As expected, FA1 shows high solubility in conventional solvents such as methanol, acetone, THF, toluene, chloroform, and hexane.

In order to increase the bio-based content of the FA1 based copolymers 4-acetoxy-3-methoxystyrene (FA2) was prepared from FA via the thermal decarbonation followed by the acetylation. In ^{1}H-NMR spectrum of FA2, all the expected signals appeared confirming the successful synthesis of FA2 [14].

4.3.2 *Copolymerization of FA1 with Styrene*

Due to the improved solubility of FA1, it is possible to carry out a bulk polymerization or a solution polymerization in concentrated conditions. At first FA1 was copolymerized with conventional styrene. Copolymerizations were conducted varying FA1 content from 10 to 90 mol% in feed. Runs 1-3, homogeneous liquids for the monomer mixture were obtained, and were copolymerized in bulk. In runs 4, and 5, 0.3 mL of toluene was added to the monomer mixture to afford the homogeneous mixture. In order to estimate the reactivity ratio of each monomer, the conditions were established so that polymerization yield was less than 5%. In run 5, methanol insoluble product was negligible. Figure 4-1 shows ^{1}H-NMR spectrum of the product (run 3). Two signals originated from silyl group appeare at 0.03 and 0.93 ppm confirming the incorporation of FA1 into the product. With the comparison of intensities of these signals to aromatic signal, the chemical compositions were determined as shown in Table 4-1. The contents of FA1 in polymers are lower than those in feed suggesting the lower monomeric reactivity than styrene due to the steric hindrance. The details of copolymerization analyses are discussed below. Propagation reactions involving FA1 radical are also retarded judging from the decrease of yield with the increase of FA1 contents.

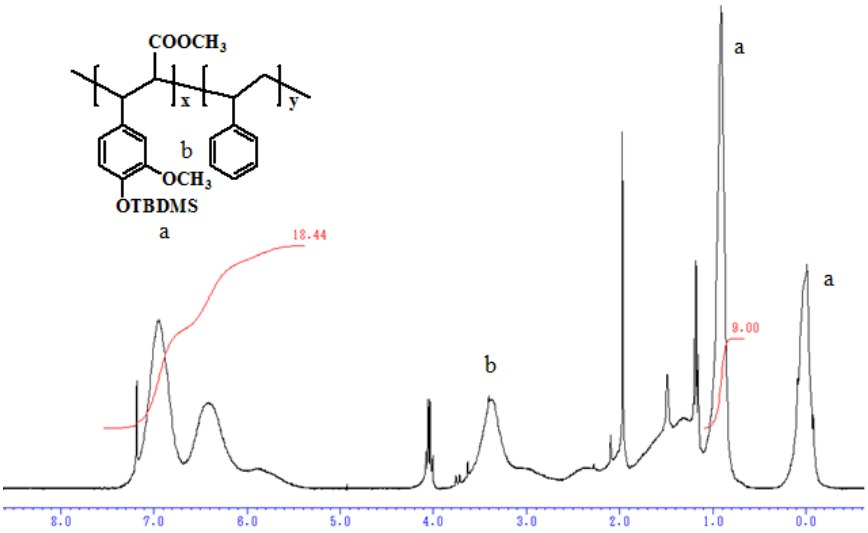

Figure 4-1 ^{1}H-NMR spectrum of copolymer (run 3) in $CDCl_3$ at 300 MHz

Table 4-1 Copolymerization of FA1 with styrene

Run	content of FA1 (mol%)		Yield (%)	M_n *2/10^3	PDI*2
	in feed	in polymer*1			
1	10.1	4.2	4.40	6.7	1.81
2	29.7	13.4	2.10	9.4	1.84
3	49.7	24.5	0.84	9.1	1.74
4*3	69.3	37.7	0.05	7.5	1.56
5*3	89.3	-	-	-	-

Total amount of monomers; 6.9 mmol, AIBN; 2mol%. Polymerizations were carried out at 80°C for 5 min.
*1 determined by ^{1}H-NMR data
*2 determined by GPC calibrated with polystyrene standards
*3 containing toluene (0.3 mL) as an additional solvent

^{13}C-NMR analyses on the copolymers were also carried out, which have been widely used to investigate the microstructure such as monomer sequence, tacticity, and regioregularity. Figures 4-2 and 4-3 show ^{13}C-NMR spectra of copolymers. As shown in Figure 4-2, characteristic signals from silyl, methoxy, carbonyl groups are observed confirming the formation of the copolymer (run 3). In Figure 4-3, expanded signals for carbonyl, and ipso carbons (from styrene, and FA1 connected to the main chain) are presented for the copolymers in runs 1 (upper), and 3 (lower).

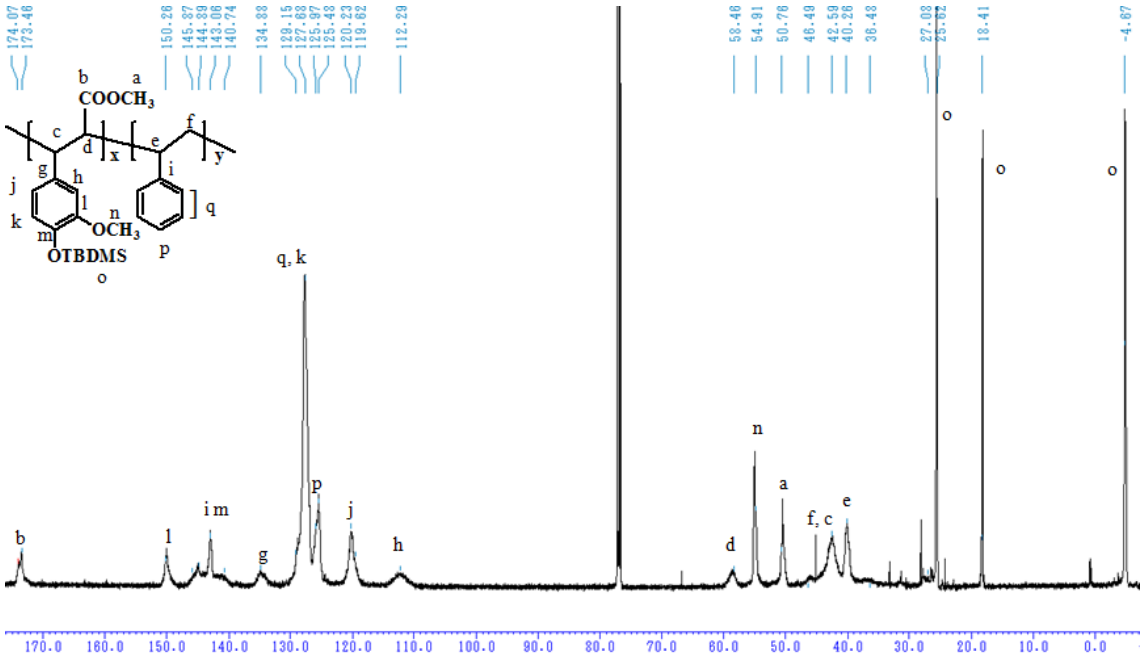

Figure 4-2 ^{13}C-NMR spectrum of copolymer (run 3) in $CDCl_3$ at 75 MHz

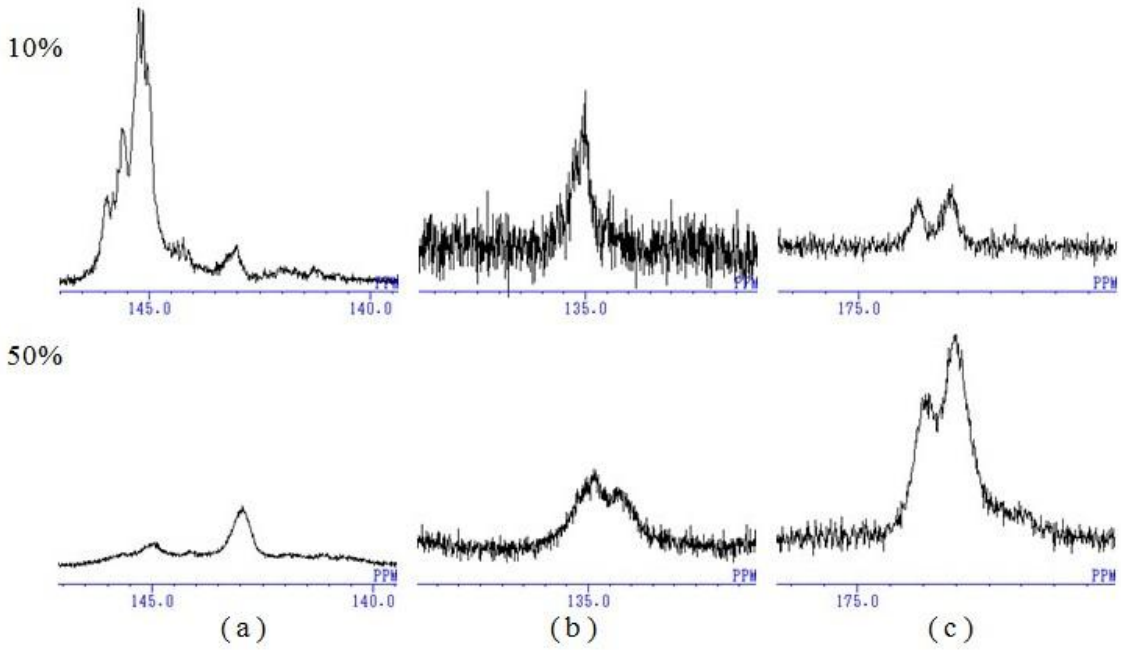

Figure 4-3 ^{13}C-NMR spectra of copolymers (run1; upper and run 3; lower) a) **i** and **m** *ipso* carbons in styrene and FA1 moieties, respectively (assignment; shown in the inserted figure in Figure 2), b) **g** ipso carbon in FA1 moiety, which is connected to the main chain), and c) **b** carbonyl carbon.

Since the styrene content of the copolymer (run 1) is high, the signal i (around 145 ppm) can be assigned to *ipso* carbon on styrene sequence taking the assignments of polystyrene into consideration (signal splitting is due to triad and pentad tacticity [18]). With the increase of FA1 content, the number of styrene sequence decreases, and broadening occurs in the copolymer with high FA1 content (run 3). Around 135 ppm, a relatively sharp signal appears for the copolymer (run 1). This signal is assigned to *ipso* carbon in FA1 moiety, which is connected to the main chain. In the copolymer (run 1), it is reasonable that this FA1 moiety is isolated in the long styrene sequence, taking low FA1 content into consideration. With the increase of FA1 content, a new signal appears at the higher magnetic field. It is speculated that this signal is caused by shortening of styrene sequence in the copolymer (run 3). Carbonyl carbon shows apparent signal splitting. As discussed above, FA1 unit is considered to be isolated in the copolymer (run 1). Therefore this splitting is not resulted from the monomer sequence. Assuming that the attack of styryl radical to FA1 at α-carbon of carbonyl group, and propagating radical is predominantly located at α-carbon of aromatic ring in FA1 [19], difference of cotacticity resulted in signal splitting. Further investigation is necessary to elucidate the microstructure of copolymers.

4.3.3 *Copolymerization of FA1 with FA2*

Styrene analogue, 4-acetoxy-3-methoxystyrene (FA2) was prepared from FA. The utilization of FA2 instead of styrene, makes it possible to increase the bio-based content of the products. Copolymerizations of FA1 with FA2 were investigated in a similar way where styrene is used as a comonomer. ^{1}H NMR of the product (run 8) is shown in Figure 4-4. Compared with the case of styrene, signals for aromatic protons are shifted to higher-magnetic field, and the resonance for acetyl proton appears around at 2.3 ppm in addition to that of silyl group. These facts strongly suggest that both monomers are incorporated in the product. At higher content of FA1, no product insoluble in methanol was

obtained. Similar tendency about dependence of monomer content on the chemical composition, and the yield is observed. Higher yield and molecular weight of copolymer were observed in the copolymerization of FA1 with FA2, suggesting the higher reactivity of FA2 than styrene.

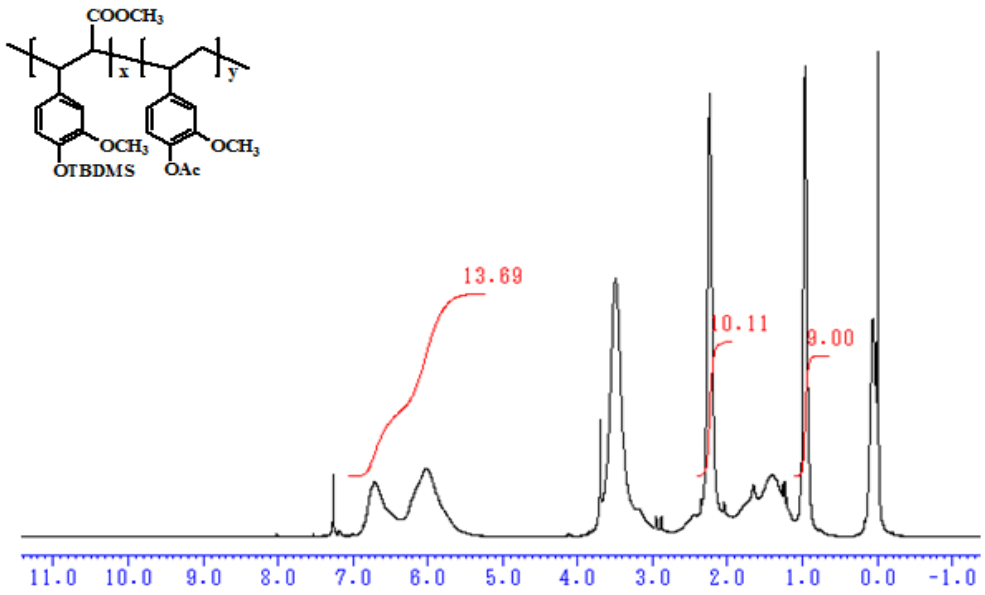

Figure 4-4 ^{1}H-NMR spectrum of copolymer (run 8) in $CDCl_3$ at 300 MHz

Table 4-2 Copolymerization of FA1 with FA2

Run	content of FA1 (mol%)		Yield (%)	M_n *2/10^3	PDI*2
	in feed	in polymer*1			
6*3	9.9	3.9	10.8	53.4	2.32
7*3	30.2	12.9	6.0	43.4	2.31
8*3	48.8	22.9	1.5	20.0	1.49
9*3	69.0	-	-	-	-
10*3	89.8	-	-	-	-

Total amount of monomers; 6.9 mmol, AIBN; 2mol%. Polymerizations were carried out at 80°C for 5 min.
*1 determined by ^{1}H-NMR data
*2 determined by GPC calibrated with polystyrene standards
*3 containing toluene (0.3 mL) as an additional solvent

4.3.4 *Copolymerization Analyses*

From the data about chemical compositions, monomer reactivity ratios (r_1, and r_2 for M_1; FA1, and M_2; styrene or FA2) were estimated using a straight line intersection method and the Fineman-Ross method. The intersection method afforded the reactivety ratios, r_1=0.13 ± 0.02, and r_2=2.47 ± 0.05 for styrene, and r_1=0.13 ± 0.01, and r_2=2.63 ± 0.02 for FA2. Figure 4-5 shows the Fineman-Ross plots for two sets of monomers. Highly reliable straight lines were obtained. Monomer reactivity ratios are estimated as r_1=0.12, and r_2=2.46 for styrene, and r_1=0.13, and r_2=2.66 for FA2, and these values are consistent with those obtained by the intersection method. Reactivity ratios of alkyl cinnamate (M1) with styrene (M2) were reported as r_1=0.10, and r_2=2.03 for methyl cinnamate, and 0.10 and 1.50 for ethyl cinnamate.[20] Similar to presented data, higher self-propagation rate of styrene was suggested.

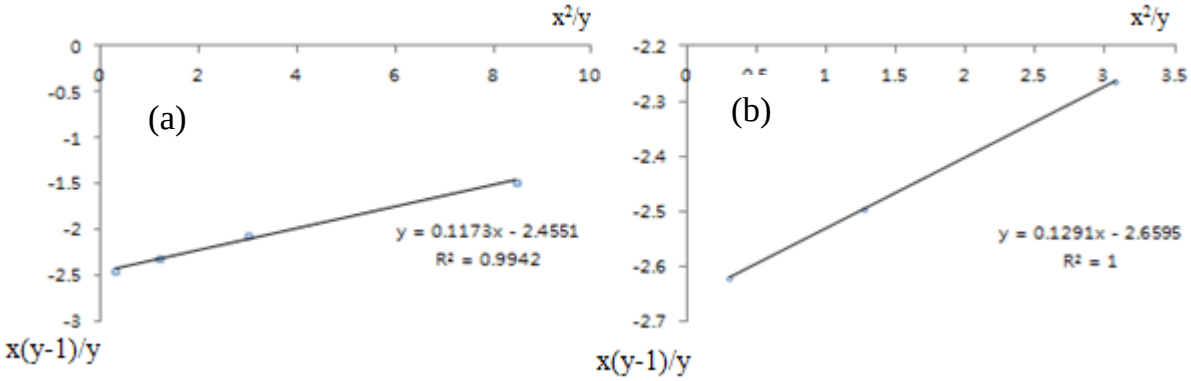

Figure 4-5 Fineman-Ross plots for (a) styrene and (b) FA2 as a monomer 2. x=[M_1]/[M_2], y=d[M_1]/d[M_2]

4.3.5 *Copolymerization of FA1 with methyl methacrylate (MMA)*

Copolymerization of FA1 with the other conventional ethylenic monomer, methyl methacrylate (MMA) was also investigated. Similar to styrene, copolymerization of FA1 with MMA in 5 different feed ratio was carried out. Table 4-3 shows the polymerization conditions and results. Contrary to styrene, it is found that FA1 cannot be copolymerized

essentially with MMA. At the low content of FA1, PMMA homopolymer was obtained. However, no polymer was produced at the high content of FA1. It is noteworthy that molecular weights of products are almost independent of the content of FA1. Therefore, the propagating end involving MMA cannot react with FA1 probably due to the fact that MMA is 1,1-disubstituted monomer, and steric hindrance between propagating radical and FA1 monomer is severe.

Table 4-3 Copolymerization of FA1 with MMA

Run	content of FA1 (mol%)		Yield (%)	M_n *2/10^3	PDI*2
	in feed	in polymer*1			
11	9.8	0	4.8	11.3	2.89
12	30.1	0	5.4	11.9	2.31
13*3	50.2	<0.1	0.9	11.4	2.43
14*3	69.2	-	-	-	-
15*3	89.9	-	-	-	-

Total amount of monomers; 6.9 mmol, AIBN; 2mol%. Polymerizations were carried out at 80^{o}C for 5 min.
*1 determined by ^{1}H-NMR data
*2 determined by GPC calibrated with polystyrene standards
*3 containing toluene (0.3 mL) as an additional solvent

4.4 Conclusion

Bio-based FA was converted to 1,2-disubstituted ethylenic monomer via methyl esterification followed by the protection of phenolic hydroxy group. Resulting monomer can be copolymerized with styrene and styrene derivative prepared from FA to afford a new class of bio-based plastics. On the other hand, in the case of the copolymerization with methyl methacrylate, homopolymer of second monomer was practically produced. In order to seek the applications, it is of necessity that the characteristics and reactivity of copolymers are further investigated.

4.5 References

1. U.B. Anvar, G. Mazza, *Food Chem*., **115**, 1542 (2009)
2. K.H. Kim, R. Tsao, R. Yang, S.W. Gnu, *Food Chem*., **95**, 466 (2006)
3. S. Mathew, T.E. Abraham, *Enzyme Microb. Technol*., **36**, 565 (2005)
4. S. Mathew, T.E. Abraham, *Crit. Rev. Microbiol*., **32**, 115 (2006)
5. M.L. Soto, A. Moure, H. Dominguez, J.C. Parajo, *J. Food Eng.*, **105**, 1 (2011)
6. F. Xu, R.C. Sun, J.X. Sun, C.F. Liu, B.H. He, J.S. Fan, *Anal. Chim. Acta*, **552**, 207 (2005)
7. N. Kumar, V. Pruthi, *Biotechnology Reports*, **4**, 86 (2014)
8. L. Mialon, A. G. Pemba, S. A. Miller, *Green Chem*., **12**, 1704 (2010)
9. I. Barbara, A. L. Flourat, F. Allais, *Eur. Polym. J*., **62**, 236 (2015)
10. M. Z. Oulame, F. Pion, S. Allauddin, K. V. S. N. Raju, P.-H. Ducrot, F. Allais, *Eur. Polym. J*., **63**, 186 (2015)
11. F. Pion , P.-H. Ducrot , F. Allais, *Macromol. Chem. Phys*., **215**, 431 (2014)
12. A. Matsumoto, T. Kubota, T. Otsu, *Macromolecules*, **23**, 4508 (1990)
13. T. Otsu, T. Yasuhara, K. Shiraishi, S. Mori, *Polym. Bull*., **12**, 449 (1984)
14. A. Hosoda, H. Mori, Y. Miyake, Y. Tanaka, S. Osaki, T. Kobata, H. Taniguchi, *Proceeding of 58th SPSJ Annual Meeting* (3Pd140), Kobe, Japan (2009)
15. M.-A. Bazin, L. El Kihel, M. Jouanne, J.-C. Lancelot, S. Rault, *Synth. Commun*., **38**, 3947 (2008)
16. K. Ogino, H. Sato, K. Tsuchiya, H. Suzuki, S. Moriguchi, *J. Chromatogr. A,* **59,** 699 (1995)
17. A. Ravve, *Principles of Polymer Chemistry*, Plelum Press, New York (1995)
18. H. Sato, Y. Tanaka, and K. Hatada, *J. Polym. Sci. Polym. Phys. Ed.*, **21**, 1667 (1983)
19. M. S. Kharasch, M. Sage, *J. Org. Chem*., **14**, 537 (1949)
20. T. Otsu, B. Yamada, T. Nozaki, *Kogyo Kagaku Zasshi*, **70**, 1941 (1967)

Chapter 5 Conclusion

This thesis deals with the development of functional bio-based polymer materials using various renewable resources such as vanillin, ferulic acid, and *p*-coumaric acid.

In the Chapter 1, general introduction for bio-based polymer materials is described.

In the Chapter 2, novel biomass based PEBO was prepared via the direct polycondensation of the synthesized monomer derived from vanillin followed by thermal cyclodehydration. Synthesized PEHA precusor was soluble in common solvents such as NMP, DMF, DMSO and H_2SO_4, while PEBO was soluble in DMSO and H_2SO_4. Improved solubility is considered to be due to the introduction of flexible ether moiety into main chain and the presence of methoxy group derived from vanillin. A simple solvent casting of precursor PEHA and the subsequent thermal treatment at 250 ℃ afforded free-standing film exhibiting flexible and tough nature. DSC analysis showed that thermal cyclodehydration of PEHA into PEBO occurred in the range of 230- 260 ℃. Prepared PEBO did not show significant weight loss before 400 ℃, indicating moderate thermal stability. The tensile strength and Young's modulus of PEBO showed 117 MPa and 5.2 GPa, respectively. These values were higher than the other ether type PBO (PEBO) analogues and commercial engineering polymers.

In the Chapter 3, the author synthesized novel Schiff base type monomer from vanillin and veratraldehyde, and homopolymerized the resulting monomer and copolymerized it with cinnamic acid derivatives (*i.e.,* CA and FA) via transesterification in order to produce wholly bio-based polymers. According to the molecular weight of homopolymers, the reactivity of this Schiff base type monomer was significantly higher than those of CA and FA. All

monomers and polymers showed photoluminescence in chloroform solution under the irradiation of 365 nm UV light. Large Stokes shift was observed in the poly(FA) solution. The photoluminescence property of poly(DAHMBA-*co*-FA) was strongly affected by FA than DAHMBA. All polymers showed high glass transition temperature which was over 100 ℃. Thermal gravimetric analysis of polymers also showed a good thermal stability until 250 ℃. Hence, these bio-based polyesters can be expected as novel engineering thermoplastics.

In the Chapter 4, bio-based FA was converted to 1,2-disubstituted ethylenic monomer via methyl esterification followed by the protection of phenolic hydroxy group. Resulting monomer can be copolymerized with styrene and styrene derivative prepared from FA to afford a new class of bio-based plastics. On the other hand, in the case of the copolymerization with methyl methacrylate, homopolymer of second monomer was practically produced. In order to seek the applications, it is of necessity that the characteristics and reactivity of copolymers are further investigated.

In the Chapter 5, conclusion of this thesis is described. The presented conclusion would facilitate the development of novel functional bio-based polymer materials. Development of functional biomass-based polymer materials have been received much attention and would play an important role to realize sustainable society in near future. It is expected that this thesis is pivotally important for further problems about bio-based polymer materials.

Achievements

Peer-reviewed Journals

1. **Hong Sun**, Yoon Deuk Young, Shinji Kanehashi, Kousuke Tsuchiya, Kenji Ogino, and Jae-Ho Sim, Accepted to *Journal of Fiber Science and Technology (JFST)*, "Synthesis and characterization of biobased poly (ether benzoxazole) derived from vanillin"

2. **Hong Sun**, Shinji Kanehashi, Kousuke Tsuchiya, and Kenji Ogino, Accepted to *Chemistry Letters*, "Synthesis and characterization of biobased polyesters derived from vanillin-based schiff base and cinnamic acid derivatives"

3. **Hong Sun**, Yoon Deuk Young, Shinji Kanehashi, Kousuke Tsuchiya, Kenji Ogino, and Jae-Ho Sim, Accepted to *Journal of Fiber Science and Technology (JFST)*, "Radical copolymeriztion of ferulic acid derivatives with ethylenic monomers"

Presentations

1. **Hong Sun** and Kenji Ogino, International Symposium on Fiber Science and Technology 2014, Tokyo, Japan, Sep.29-Oct.1, 2014.

2. **Hong Sun** and Kenji Ogino, The Society of Fiber Science and Technology Annual Meeting 2015, Tokyo, Japan, June.10-12, 2015